dysplastic nodules and well-differentiated HCC is variable, the signal intensity of these nodules may also vary after administration of SPIO.[57,64] It has been suggested that the extent of SPIO uptake may reflect the degree of Kupffer cell function (**Fig. 20**).[65] Signal intensity characteristics of dysplastic nodules after administration of SPIO also overlap with those of regenerative nodules and well-differentiated HCC, and uptake of SPIO into these nodules may cause a decrease in detection.

Regenerative nodules generally have normal hepatocellular function and therefore demonstrate uptake of hepatocellular contrast agents such as Gd-EOB-DTPA. As dedifferentiation proceeds, the number of expressed organic anion transporters decreases, with a resulting progressive decrease in the uptake of hepatocellular agents.[66] It is considered that the appearance of HCC at hepatocyte-selective phases with hepatocellular agents is dependent on the degree of tumor differentiation. However, hepatocytes in well-differentiated HCC may retain enough hepatocellular function to take up hepatocellular agents, and hence may be overlooked at this phase of imaging, or appear similar to a regenerative or dysplastic nodule (see **Table 4**).

In the authors' experience, most well-differentiated HCCs diagnosed by needle biopsy are clearly observed as hypointense to liver at hepatocyte-selective phases on Gd-EOB-DTPA–enhanced MR imaging (**Fig. 21**). Nevertheless, some well-differentiated HCCs are observed as isointense or hyperintense. Conclusive differentiation of dysplastic nodules from well-differentiated HCCs appears difficult (**Fig. 22**). Moreover, the diagnostic differentiation of dysplastic nodules from other cirrhosis-associated hepatocellular nodules may be difficult even on histopathologic analysis, and the use of molecular genetics-based techniques may be necessary in future.[61]

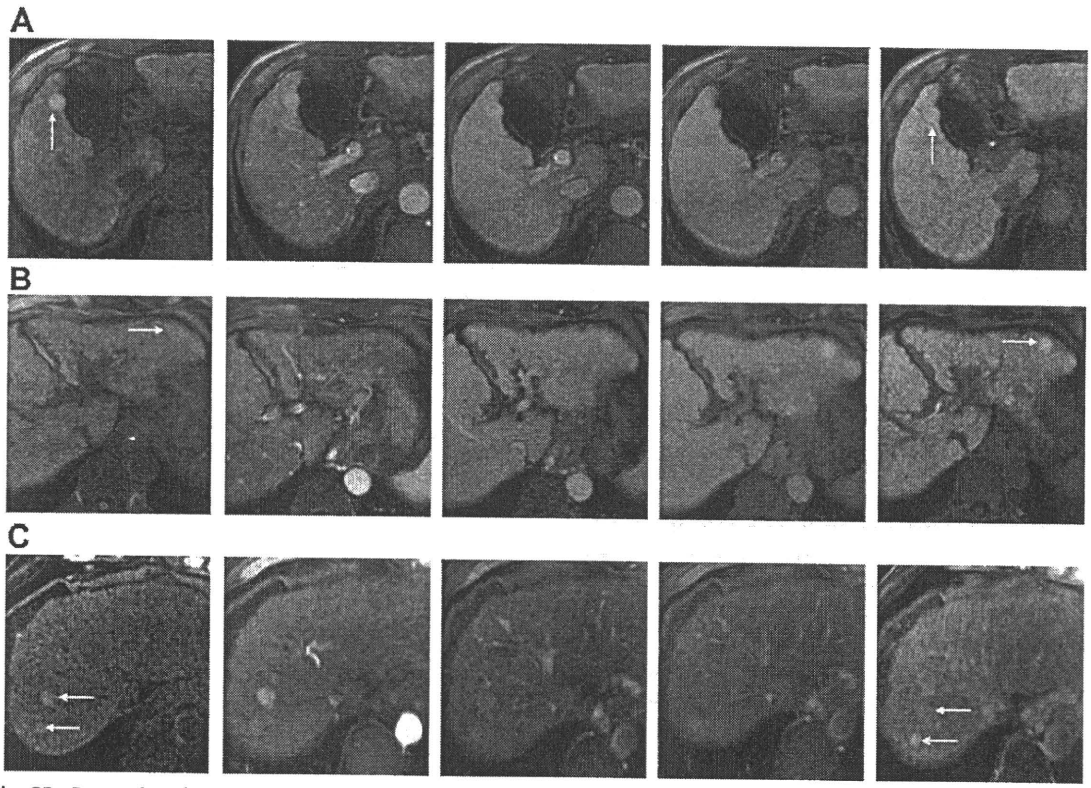

Fig. 22. Dynamic enhancement patterns of a low-grade dysplastic nodule (*A*), high-grade dysplastic nodule (*B*), and well-differentiated HCCs (*C*) in axial T1-weighted fat-saturated 3D GRE images (TR/TE = 3.6/1.7 ms, flip angle = 15°), presenting before and in the arterial phase, portal phase, equilibrium phase, and hepatocyte-selective phase after intravenous injection of Gd-EOB-DTPA. In the hepatocyte-selective phase, each nodule is observed as isointense or hyperintense owing to the uptake of hepatocellular agents (*arrows*). In series (*C*), both nodules were well-differentiated HCCs. In the hepatocyte-selective phase, both HCCs are observed as isointense and hyperintense, respectively. All these HCCs were diagnosed by needle biopsy.

REFERENCES

1. Mortele KJ, Ros PR. MR imaging in chronic hepatitis and cirrhosis. Semin Ultrasound CT MR 2002;23(1): 79–100.
2. Popper H. Pathologic aspects of cirrhosis. A review. Am J Pathol 1978;87:228–58.
3. Garcia-Tsao G, Lim JK. Members of Veterans Affairs Hepatitis C Resource Center Program. Management and treatment of patients with cirrhosis and portal hypertension: recommendations from the Department of Veterans Affairs Hepatitis C Resource Center Program and the National Hepatitis C Program. Am J Gastroenterol 2009;104(7):1802–29.
4. Sorrell MF, Belongia EA, Costa J, et al. National Institutes of Health Consensus Development Conference Statement: management of hepatitis B. Ann Intern Med 2009;150:104–10.
5. Global surveillance and control of hepatitis C. Report of a who consultation organized in collaboration with the viral hepatitis prevention board, Antwerp, Belgium. J Viral Hepat 1999;6:35–47.
6. Davis GL, Albright JE, Cook SF, et al. Projecting future complications of chronic hepatitis C in the United States. Liver Transpl 2003;9:331–8.
7. Afdhal NH. The natural history of hepatitis C. Semin Liver Dis 2004;24(Suppl 2):3–8.
8. Maher JJ. Alcoholic liver disease. In: Feldman M, Friedman LS, Sleisenger MH, editors. Gastrointestinal and liver disease, vol. II. Philadelphia: Saunders; 2002. p. 1375–91.
9. Breitkopf K, Nagy LE, Beier JI, et al. Current experimental perspectives on the clinical progression of alcoholic liver disease. Alcohol Clin Exp Res 2009; 33:1647–55.
10. Greenfield V, Cheung O, Sanyal AJ. Recent advances in nonalcoholic fatty liver disease. Curr Opin Gastroenterol 2008;24(3):320–7.
11. Itoh H, Sakai T, Takahashi N, et al. Periportal high intensity on T2-weighted MR images in acute viral hepatitis. J Comput Assist Tomogr 1992;16:564–7.
12. Matsui O, Kadoya M, Takashima T, et al. Intrahepatic periportal abnormal intensity on MR images: an indication of various hepatobiliary diseases. Radiology 1989;171:335–8.
13. Fisher MR, Gore RM. Computed tomography in the evaluation of cirrhosis and portal hypertension. J Clin Gastroenterol 1985;7:173–81.
14. Ito K, Mitchell DG, Gabata T. Enlargement of hilar periportal space: a sign of early cirrhosis at MR imaging. J Magn Reson Imaging 2000;11:136–40.
15. Ito K, Mitchell DG. Imaging diagnosis of cirrhosis and chronic hepatitis. Intervirology 2004;47:134–43.
16. Ito K, Mitchell DG, Siegelman ES. Cirrhosis: MR imaging features. Magn Reson Imaging Clin N Am 2002;10:75–92.
17. Lafortune M, Matricardi L, Denys A, et al. Segment 4 (the quadrate lobe): a barometer of cirrhotic liver disease at US. Radiology 1998;206:157–60.
18. Ito K, Mitchell DG, Gabata T, et al. Expanded gallbladder fossa: simple MR imaging sign of cirrhosis. Radiology 1999;211:723–6.
19. Ito K, Mitchell DG, Kim MJ, et al. Right posterior hepatic notch sign: a simple diagnostic MR finding of cirrhosis. J Magn Reson Imaging 2003;18:561–6.
20. Okazaki H, Ito K, Fujita T, et al. Discrimination of alcoholic from virus-cirrhosis on MR imaging. AJR Am J Roentgenol 2000;175:1677–81.
21. Ito K, Mitchell DG, Outwater EK, et al. Primary sclerosing cholangitis: MR imaging features. AJR Am J Roentgenol 1999;172(6):1527–33.
22. Brancatelli G, Federle MP, Ambrosini R. Cirrhosis: CT and MR imaging evaluation. Eur J Radiol 2007; 61(1):57–69.
23. Wenzel JS, Donohoe A, Ford KL 3rd, et al. Primary biliary cirrhosis: MR imaging findings and description of MR imaging periportal halo sign. AJR Am J Roentgenol 2001;176:885–9.
24. Kobayashi S, Matsui O, Gabata T, et al. MRI findings of primary biliary cirrhosis: correlation with Scheuer histologic staging. Abdom Imaging 2005;30(1): 71–6.
25. Martí-Bonmatí L. MR contrast agents in hepatic cirrhosis and chronic hepatitis. Semin Ultrasound CT MR 2002;23(1):101–13.
26. Vilgrain V. Ultrasound of diffuse liver disease and portal hypertension. Eur Radiol 2001;11:1563–77.
27. Van Beers BE, Leconte I, Materne R, et al. Hepatic perfusion parameters in chronic liver disease: dynamic CT measurements correlated with disease severity. AJR Am J Roentgenol 2001;176:667–73.
28. Semelka RC, Chung JJ, Hussain SM, et al. Chronic hepatitis: correlation of early patchy and late linear enhancement patterns on gadolinium-enhanced MR images with histopathology: initial experience. J Magn Reson Imaging 2001;13:385–91.
29. Faria SC, Ganesan K, Mwangi I, et al. MR imaging of liver fibrosis: current state of the art. Radiographics 2009;29(6):1615–35.
30. Yeh MM, Brunt EM. Pathology of nonalcoholic fatty liver disease. Am J Clin Pathol 2007;128(5):837–47.
31. Bedossa P, Dargere D, Paradis V. Sampling variability of liver fibrosis in chronic hepatitis C. Hepatology 2003;38:1449–57.
32. Blci NC, Semelka RC. Contrast agents for MR imaging of the liver. Radiol Clin North Am 2005; 43(5):887–98.
33. Lucidarme O, Baleston F, Cadi M, et al. Non-invasive detection of liver fibrosis: Is superparamagnetic iron oxide particle-enhanced MR imaging a contributive technique? Eur Radiol 2003;13(3):467–74.
34. Aguirre DA, Behling CA, Alpert E, et al. Liver fibrosis: noninvasive diagnosis with double contrast

material-enhanced MR imaging. Radiology 2006; 239:425–37.
35. Martí-Bonmatí L, Lonjedo E, Poyatos C, et al. MnDPDP enhancement characteristics and differentiation between cirrhotic and noncirrhotic livers. Invest Radiol 1998;33(10):717–22.
36. Murakami T, Baron RL, Federle MP, et al. Cirrhosis of the liver: MR imaging with mangafodipir trisodium (Mn-DPDP). Radiology 1996;198(2):567–72.
37. Muthupillai R, Lomas DJ, Rossman PJ, et al. Magnetic resonance elastography by direct visualization of propagating acoustic strain waves. Science 1995;269:1854–7.
38. Muthupillai R, Ehman RL. Magnetic resonance elastography. Nat Med 1996;2:601–3.
39. Yin M, Talwalkar JA, Glaser KJ, et al. Assessment of hepatic fibrosis with magnetic resonance elastography. Clin Gastroenterol Hepatol 2007;5(10): 1207–13.
40. Taouli B, Tolia AJ, Losada M, et al. Diffusion-weighted MRI for quantification of liver fibrosis: preliminary experience. AJR Am J Roentgenol 2007;189:799–806.
41. Boulanger Y, Amara M, Lepanto L, et al. Diffusion-weighted MR imaging of the liver of hepatitis C patients. NMR Biomed 2003;16:132–6.
42. Luciani A, Vignaud A, Cavet M, et al. Liver cirrhosis: intravoxel incoherent motion MR imaging—pilot study. Radiology 2008;249:891–9.
43. Koinuma M, Ohashi I, Hanafusa K, et al. Apparent diffusion coefficient measurements with diffusion-weighted magnetic resonance imaging for evaluation of hepatic fibrosis. J Magn Reson Imaging 2005;22:80–8.
44. Jalan R, Taylor-Robinson SD, Hodgson HJF. In vivo hepatic magnetic resonance spectroscopy: clinical or research tool? J Hepatol 1999;25:414–24.
45. Khan SA, Cox IJ, Hamilton G, et al. In vivo and in vitro nuclear magnetic resonance spectroscopy as a tool for investigating hepatobiliary disease: a review of H and P MRS applications. Liver Int 2005;25:273–81.
46. Munakata T, Griffiths RD, Martin PA, et al. An in vivo ^{31}P MRS study of patients with liver cirrhosis: progress towards a non-invasive assessment of disease severity. NMR Biomed 1993;6:168–72.
47. Van Wassenaer-van Hall HN, van der Grond J, van Hattum J, et al. ^{31}P magnetic resonance spectroscopy of the liver: correlation with standardized serum, clinical, and histological changes in diffuse liver disease. Hepatology 1995;21:443–9.
48. Menon DK, Sargentoni J, Taylor-Robinson SD, et al. Effect of functional grade and etiology on in vivo hepatic phosphorus-31 magnetic resonance spectroscopy in cirrhosis: biochemical basis of spectral appearances. Hepatology 1995; 21:417–27.
49. Cho SG, Kim MY, Kim HJ, et al. Chronic hepatitis: in vivo proton MR spectroscopic evaluation of the liver and correlation with histopathologic findings. Radiology 2001;221:740–6.
50. Coleman WB. Mechanisms of human hepatocarcinogenesis. Curr Mol Med 2003;3(6):573–88.
51. Lee RG. Fibrosis and cirrhosis. In: Lee RG, editor. Diagnostic liver pathology. St Louis (MO): Mosby-Year Book, Inc; 1994. p. 281–308.
52. Krinsky GA, Lee VS. MR imaging of cirrhotic nodules. Abdom Imaging 2000;25:471–82.
53. Zhang J, Krinsky GA. Iron-containing nodules of cirrhosis. NMR Biomed 2004;17(7):459–64.
54. Seale MK, Catalano OA, Saini S, et al. Hepatobiliary-specific MR contrast agents: role in imaging the liver and biliary tree. Radiographics 2009;29(6): 1725–48.
55. Lim JH, Kim EY, Lee WJ, et al. Regenerative nodules in liver cirrhosis: findings at CT during arterial portography and CT hepatic arteriography with histopathologic correlation. Radiology 1999;210(2): 451–8.
56. International Consensus Group for Hepatocellular Neoplasia. Pathologic diagnosis of early hepatocellular carcinoma: a report of the international consensus group for hepatocellular neoplasia. Hepatology 2009;49(2):658–64.
57. Hanna RF, Aguirre DA, Kased N, et al. Cirrhosis-associated hepatocellular nodules: correlation of histopathologic and MR imaging features. Radiographics 2008;28(3):747–69.
58. Amano S, Ebara M, Yajima T, et al. Assessment of cancer cell differentiation in small hepatocellular carcinoma by computed tomography and magnetic resonance imaging. J Gastroenterol Hepatol 2003; 18:273–9.
59. Ebara M, Fukuda H, Kojima Y, et al. Small hepatocellular carcinoma: relationship of signal intensity to histopathologic findings and metal content of the tumor and surrounding hepatic parenchyma. Radiology 1999;210:81–8.
60. Matsui O, Kadoya M, Kameyama T, et al. Benign and malignant nodules in cirrhotic livers: distinction based on blood supply. Radiology 1991;178:493–7.
61. Willatt JM, Hussain HK, Adusumilli S, et al. MR Imaging of hepatocellular carcinoma in the cirrhotic liver: challenges and controversies. Radiology 2008; 247(2):311–30.
62. Mitchell DG, Rubin R, Siegelman ES, et al. Hepatocellular carcinoma within siderotic regenerative nodules: appearance as a nodule within a nodule on MR images. Radiology 1991;178(1):101–3.
63. Goshima S, Kanematsu M, Matsuo M, et al. Nodule-in-nodule appearance of hepatocellular carcinomas: comparison of gadolinium-enhanced and ferumoxides-enhanced magnetic resonance imaging. J Magn Reson Imaging 2004;20(2):250–5.

64. Lim JH, Choi D, Cho SK, et al. Conspicuity of hepatocellular nodular lesions in cirrhotic livers at ferumoxides-enhanced MR imaging: importance of Kupffer cell number. Radiology 2001;220(3):669–76.
65. Tonan T, Fujimoto K, Azuma S, et al. Evaluation of small (< or = 2 cm) dysplastic nodules and well-differentiated hepatocellular carcinomas with ferucarbotran-enhanced MRI in a 1.0-T MRI unit: utility of T2*-weighted gradient echo sequences with an intermediate-echo time. Eur J Radiol 2007; 64(1):133–9.
66. Gandi SN, Brown MA, Wong JG, et al. MR contrast agents for liver imaging: what, when, how. Radiographics 2006;26:1621–36.

The American Journal of Pathology, Vol. 176, No. 1, January 2010

DOI: 10.2353/ajpath.2010.090242

Gastrointestinal, Hepatobiliary and Pancreatic Pathology

Pigment Epithelium-Derived Factor Inhibits Lysosomal Degradation of Bcl-xL and Apoptosis in HepG2 cells

Takumi Kawaguchi,*†‡ Sho-ichi Yamagishi,§ Minoru Itou,† Koji Okuda,¶ Shuji Sumie,† Ryoko Kuromatsu,† Masahiro Sakata,† Mitsuhiko Abe,† Eitaro Taniguchi,†‡ Hironori Koga,†‡ Masaru Harada,‖ Takato Ueno,†‡ and Michio Sata*†‡

From the Departments of Digestive Disease Information and Research, Medicine,† Pathophysiology and Therapeutics of Diabetic Vascular Complications,§ and Surgery,¶ Kurume University School of Medicine, Kurume; the Research Center for Innovative Cancer Therapy,‡ and the 21st Century Center of Excellence, Program for Medical Science, Kurume University, Kurume; and the Third Department of Internal Medicine,‖ School of Medicine, University of Occupational and Environmental Health, Kurume, Japan*

Pigment epithelium-derived factor (PEDF) has several biological actions on tumor cells, but its effects are cell-type dependent. The aim of this study was to examine the pathophysiological role of PEDF in hepatocellular carcinoma (HCC). PEDF expression was examined in various hepatoma cell lines and human HCC tissues, and was seen in various hepatoma cell lines including HepG2 cells. In human HCC tissues, PEDF expression was higher than in adjacent non-HCC tissues. In addition, serum PEDF levels were higher in HCC patients than in non-HCC patients, and curative treatment of HCC caused significant reductions in serum PEDF levels compared with pretreatment levels. *In vitro* experiments, camptothecin (CPT) was used to induce apoptosis and the effect of PEDF was investigated by knockdown of the *PEDF* gene in CPT-treated HepG2 cells. Knockdown of the *PEDF* gene enhanced CPT-induced apoptosis, simultaneously down-regulating Bcl-xL expression in HepG2 cells. Expression of apoptosis-related molecules and effects of bafilomycin A1 on CPT-induced apoptosis were also examined in *PEDF* gene knockdown HepG2 cells. Treatment with bafilomycin A1 suppressed CPT-induced decreases in Bcl-xL expression and increases in apoptosis in *PEDF* gene knockdown HepG2 cells. PEDF may, therefore, exert anti-apoptotic effects through inhibition of lysosomal degradation of Bcl-xL in CPT-treated HepG2 cells. ***(Am J Pathol 2010, 176:168–176; DOI: 10.2353/ajpath.2010.090242)***

Hepatocellular carcinoma (HCC) is a common cancer that causes nearly 1 million deaths a year worldwide.[1] The incidence of HCC is predicted to continue to increase over the next 30 years.[2] To develop new therapeutic strategies, it is important to elucidate molecular mechanisms underlying hepatocarcinogenesis.

Pigment epithelium-derived factor (PEDF) is a 50-kDa glycoprotein initially isolated from fetal human retinal pigment epithelial cells.[3] PEDF exerts a range of biological effects depending on the type of the target cell. PEDF induces apoptosis of endothelial cells and results in inhibition of neovascularization.[4] Overexpression of PEDF causes a reduction in tumor microvessel density and subsequent anti-tumor effects in pancreatic adenocarcinoma and melanoma cells.[5,6] In contrast to its effects in endothelial cells, PEDF causes the opposite effect in other types of cells. PEDF protects granule cells against both natural and potassium-induced apoptosis through activation of prosurvival genes.[7] In cultured retinal pericytes, PEDF inhibits oxidative stress-induced apoptosis through an increased ratio of B-cell leukemia/lymphoma

Supported in part by the Vehicle Racing Commemorative Foundation, a Grant-in-Aid for Young Scientists (number 19790643 to T.K.) and a Grant-in-Aid for Scientific Research (number 21590865 to M.S.) from the Ministry of Education, Culture, Sports, Science, and Technology of Japan, by Health and Labour Sciences Research Grants for Research on Hepatitis from the Ministry of Health, Labour, and Welfare of Japan, and by a Grant for Cancer Research from Fukuoka Cancer Society.

Accepted for publication September 10, 2009.

Supplemental material for this article can be found on *http://ajp.amjpathol.org*.

Address reprint requests to Takumi Kawaguchi, M.D., Ph.D., Department of Digestive Disease Information and Research, Division of Gastroenterology, Department of Medicine, Kurume University School of Medicine, 67 Asahi-machi, Kurume 830-0011, Japan. E-mail: takumi@med.kurume-u.ac.jp.

2 (Bcl-2)-associated X protein (bax) to bcl-2 mRNA levels with subsequent activation of caspase-3.[8,9] PEDF also inhibits light-induced apoptotic processes in photoreceptor cells *in vivo*.[10,11]

HCC is a hypervascular solid tumor, in which neovascularization plays an important role in disease progression and prognosis. However, changes in PEDF expression in human HCC have never been investigated and therefore, it is unclear whether PEDF is a useful target for therapeutic strategies in patients with HCC. Dysregulation of apoptosis is also deeply involved in hepatocarcinogenesis. Although HCC is known to be resistant to apoptosis,[12] it remains unknown whether PEDF has anti-apoptotic effects in HCC.

Thus, PEDF is a multifunctional protein with opposing activities, apoptotic and anti-apoptotic activities. These disparate effects depend on cell type. The aims of the present study were to investigate changes in PEDF expression and the role of PEDF in HCC.

Materials and Methods

Materials

All reagents were purchased from Wako Pure Chemical Industries (Osaka, Japan) unless otherwise indicated.

Cell Lines

Human hepatoma cell lines, HepG2, Hep3B, Huh-7, PLC/PRF/5, HLF and SK-Hep1, and the human hepatocyte cell line, OUMS-29,[13,14] were maintained in Dulbecco's modified Eagle's medium supplemented with 10% fetal bovine serum, penicillin (100 U/ml), and streptomycin (100 U/ml) at 37°C in a humidified atmosphere containing 5% CO_2 as previously described.[15] Because PEDF is present in fetal bovine serum, each cell line was incubated for 48 hours with Dulbecco's modified Eagle's medium without fetal bovine serum to examine PEDF expression in culture medium.

Human Samples

We obtained six pairs of HCCs and adjacent non-HCC liver tissues at the time of surgical resection for HCC. All tissues were stored at −80°C until used. Serum samples were obtained from cirrhotic patients with non-HCC (n = 25) or HCC (n = 110). Paired serum samples were also obtained from patients with HCC before and after complete treatment with surgical resection or percutaneous radiofrequency ablation (n = 15). All serum samples were stored at −80°C until used. Informed consent in writing was obtained from each patient and the study protocol conformed to the ethical guidelines of the 1975 Declaration of Helsinki as reflected in a prior approval by the institutional review committee.

RT-PCR

From each cell line or each tissue, total RNA was isolated with TRIzol reagent (Invitrogen, Carlsbad, CA). Two hundred fifty nanograms of RNA was used as a template for RT-PCR as previously described.[16] Expression of mRNA was evaluated by using a pair of unique primers for human *PEDF* (sense 5′-CCGGGCTCTCTACTATGACTTGAT-3′ and antisense 5′-ACGGTCCTCTCTTGATCCAAGTAG-3′), *β-actin* primer pair (Promega, Madison, WI), or *cyclophilin* (sense 5′-CCCACCGTGTTCTTCGAC-3′ and antisense 5′-ATCTTCTGCTGGTCTTGCC-3′). The cycle numbers (24 cycles for *PEDF*; 20 cycles for *β-actin*; 22 cycles for *cyclophilin*) for amplification were chosen in the linear range. The above conditions were determined by plotting signal intensities as functions of the template amounts and cycle numbers, and reactions proceeded linearly.

Immunohistochemistry

Cell lines were fixed with 100% acetone at −20°C for 20 minutes. Nonfixed human tissues were sectioned at a thickness of 6 μm and fixed with 100% acetone at −20°C for 20 minutes. Cells or sections were washed three times for 5 minutes each in PBS (pH 7.4, 130 mmol/L NaCl, 2 mmol/L NaH_2PO_4, and 7 mmol/L Na_2HPO_4) and then blocked with 10% skim milk in PBS for 30 minutes. Cells or sections were incubated overnight at 4°C with the monoclonal antibody to human PEDF (Chemicon International, Temecula, CA or TransGenic, Kumamoto, Japan) diluted 1:100 in PBS. After several washes with PBS, cells or sections were incubated for 1 hour with the secondary antibody, horseradish peroxidase-labeled anti-mouse IgG (Amersham Biosciences, Piscataway, NJ), or a fluorescein isothiocyanate (FITC)-conjugated goat anti-mouse IgM (Cappel, Aurora, OH) diluted 1:100 in PBS at room temperature. Subsequently, cells or sections were washed with PBS. Immunostaining for PEDF was developed with 3,3′-diaminobenzidine or a confocal laser scanning microscope (FluoView FV 300; Olympus, Tokyo, Japan). In addition, propidium iodide was used concomitantly for nuclear staining. The stored images were overlaid to create a single integrated image referred to as a "volume projection" by using the manufacturer's proprietary software (Olympus) as previously described.[17]

Immunoblotting and Quantitation

Conditioned media were quantitated by using DC protein assay kit (Bio-Rad Laboratories, Hercules, CA) according to the manufacturer's instruction. Proteins were resolved by using 10% SDS-polyacrylamide gel electrophoresis gel. Following electrophoresis, proteins were transblotted onto polyvinylidene difluoride membranes (PolyScreen, PerkinElmer Life Sciences, Waltham, MA). The membranes were blocked with 5% fat-free skim milk powder in Tris-buffered saline containing 0.02% (v/v) Tween 20. The primary antibodies were monoclonal antibodies to human PEDF (Chemicon or TransGenic), p53 (Cell Signaling Technology, Danvers, MA), phospho-p53 (Ser46) (Cell Signaling Technology), Akt (Cell Signaling Technology), phospho-Akt (Cell Signaling Technology), cyclin D1 (Cell Signaling Technology), Bax (Cell Signaling Technology),

survivin (Cell Signaling Technology), or Bcl-xL (Cell Signaling Technology). The bound antibodies were detected with horseradish peroxidase-labeled anti-mouse or anti-rat IgG (Amersham Biosciences) by using an enhanced chemiluminescence detection system (ECL advanced kit, Amersham Biosciences) as previously described.[18] A positive signal from the target proteins was visualized by using an image analyzer LAS-1000 plus (Fujifilm, Tokyo, Japan). Band intensities were determined by using the Scion Image (Scion Corporation, Frederick, MD). Values were based on four different experiments.

Assay for Serum or Medium PEDF

Serum or medium PEDF measurements were performed with a modified competitive enzyme-linked immunosorbent assay (ELISA) as previously described.[19] To dissociate PEDF from binding-proteins, 50 μl of serum or medium was pretreated with 200 μl of 8 M urea for 1 hour. Then, 100-μl aliquots of standard recombinant human PEDF proteins (Chemicon International) or 50-fold diluted serum were added to wells that had been precoated with an anti-PEDF monoclonal antibody (TransGenic). Then, 50 μl of biotinylated anti-human PEDF polyclonal antibody (R and D Systems, Minneapolis, MN) was added to each well, and the plate was read at 450 nm by using a microplate reader.

Small Interfering RNA-Mediated Gene Knockdown and Evaluation of Apoptosis

PEDF gene was knocked down by using small interfering RNA (siRNA) in HepG2 cells. HepG2 cells were plated together with siRNA (individual siRNA serpinF1 or negative control number 2; Ambion, Austin, TX)-siPORT NeoFX complexes. Twenty-four hours later, siRNA-siPORT NeoFX complexes were removed by replacing them with basal medium containing 1% serum and an apoptosis inducer, camptothecin (CPT; 2 μmol/L) and then cells were incubated for 24 hours. In some experiments, 10 μmol/L of carbobenzoxy-L-leucyl-L-leucyl-L-leucinal (MG132; Peptide Institute, Osaka, Japan), a proteasomal proteolysis inhibitor or 100 nmol/L of bafilomycin A1, a lysosomal proteolysis inhibitor was mixed with CPT. Apoptosis was evaluated by visualization of caspase activity by using a FITC-labeled carbobenzoxy-valyl-alanyl-aspartyl-fluoromethylketone (CaspACE FITC-VAD-fmk *in situ* marker; Promega) according to the manufacturer's instructions and quantified by terminal deoxynucleotidyl transferase-mediated dUTP nick-end labeling assay by using the Cell Death Detection ELISA kit (Roche Applied Science, Mannheim, Germany) according to the manufacturer's instructions. Knockdown of the *PEDF* gene was verified by semiquantitative RT-PCR and by measuring medium PEDF levels.

Statistical Analysis

All data are expressed as mean ± SD. Comparisons between any two groups were performed by using the Mann-Whitney *U* test. Comparisons among multiple groups were analyzed by using the Kruskal-Wallis analysis of variance. A P value <0.05 was considered statistically significant.

Results

PEDF mRNA and PEDF Expression in Human Hepatoma Cell Lines

No expression and weak expression of PEDF mRNA were seen in HLF and SK-Hep1 cells, respectively. However, expression of PEDF mRNA was seen in OUMS-29, HepG2, Hep3B, Huh-7, and PLC/PRF/5 cells (Figure 1A). Intracellular expression of PEDF was seen in OUMS-29, HepG2, Hep3B, Huh-7, and PLC/PRF/5 cells, but not in HLF and SK-Hep1 cells (Figure 1B). Secreted PEDF in the culture medium was evaluated by using two different primary antibodies. Expression of PEDF was seen in the culture medium of HepG2, Hep3B, Huh-7, and PLC/PRF/5 cells, but not in that of HLF, OUMS-29, and SK-Hep1 cells (Figure 1C, upper column). Similar results were obtained when a different primary antibody was used (Figure 1C, lower column).

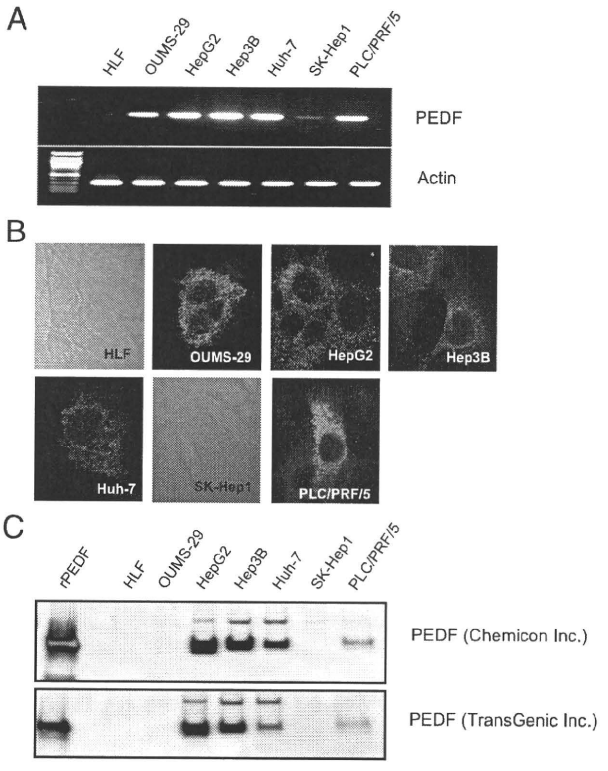

Figure 1. Expression of PEDF mRNA and actin mRNA as a control in various human hepatoma cell lines (**A**), intracellular expression of PEDF (**B**), and secreted PEDF into the culture medium (**C**) were evaluated by RT-PCR, immunohistochemistry, and immunoblotting, respectively. In HLF and SK-Hep1 cells, PEDF expression was negative and cell morphology was demonstrated by phase contrast (**B**).

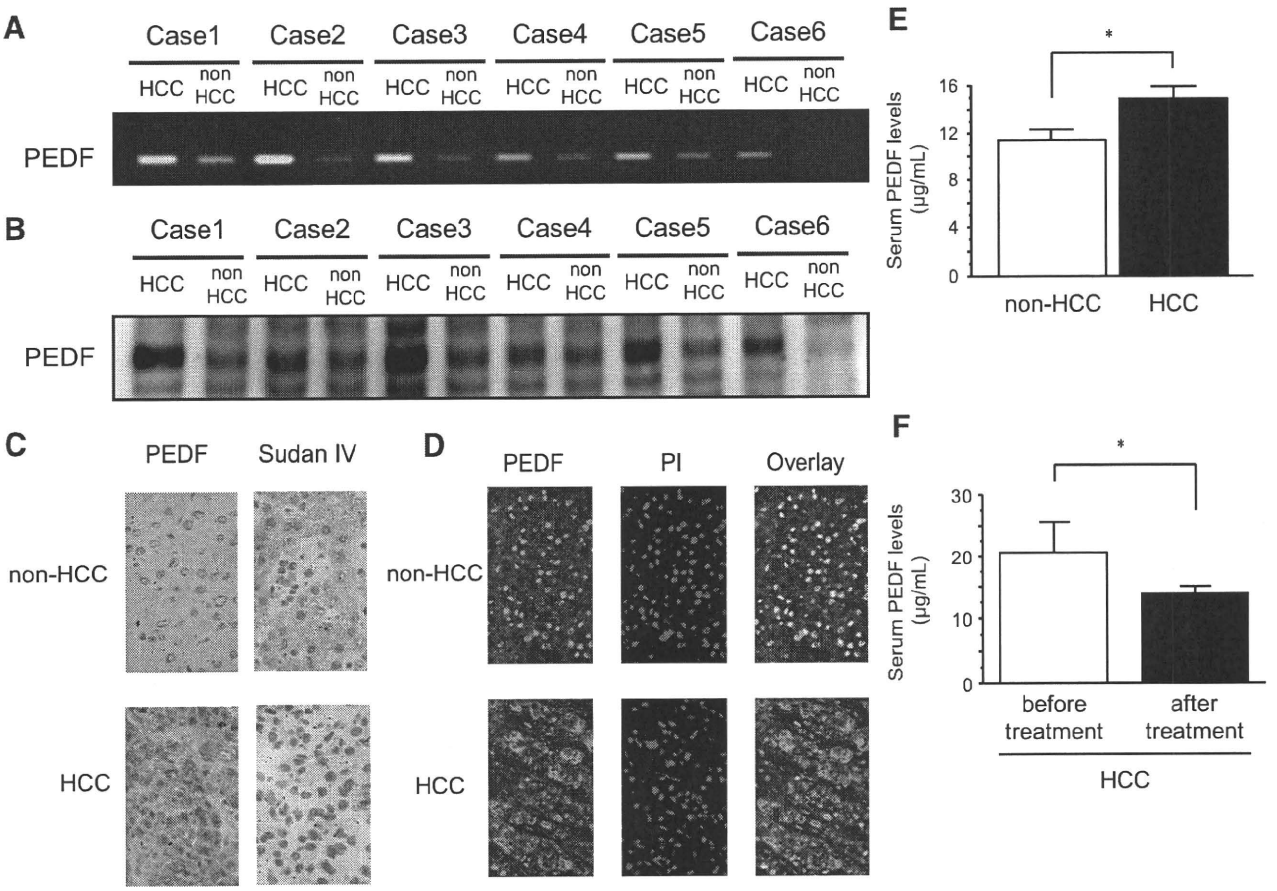

Figure 2. In human HCC tissues and adjacent non-HCC liver tissues, expression of PEDF mRNA ($n = 6$) (**A**) and PEDF ($n = 6$) (**B**) were evaluated by RT-PCR and immunoblotting, respectively. The distribution of PEDF was examined by immunostaining. Immunostaining for PEDF was developed with 3,3′-diaminobenzidine (**C**) and lipid accumulation was evaluated by Sudan IV staining (**C**). The distribution of PEDF was examined by a confocal laser scanning microscopy. Green color indicates expression of PEDF and red color indicates propidium iodide, a marker for the nucleus. Yellow color indicates co-localization of PEDF and propidium iodide (**D**). Serum PEDF levels were measured in non-HCC patients ($n = 25$) or HCC patients ($n = 110$) with a competitive ELISA (**E**). Changes in serum PEDF levels after HCC treatment were examined in HCC patients treated with surgical resection or percutaneous radiofrequency ablation ($n = 15$) (**F**). $^*P < 0.01$.

PEDF mRNA and PEDF Expression in Human Liver Tissues and Serum Samples

Expression of PEDF mRNA was higher in HCC tissue than in non-HCC tissue in all cases (Figure 2A). Similar to expression of PEDF mRNA, expression of PEDF was higher in HCC tissue than in non-HCC tissue in all cases (Figure 2B). When PEDF was visualized by 3,3′-diaminobenzidine, expression of PEDF was seen in nuclei of hepatocytes and mainly in the cytoplasm of HCC where no lipid accumulation was seen by Sudan IV staining (Figure 2C). Similar results were obtained by confocal laser scanning microscopy. In hepatocytes, PEDF (green color) was colocalized with propidium iodide (red color), showing a yellow color in the overlay image (Figure 2D, upper column). However, in HCC, PEDF (green color) was dissociated with propidium iodide (red color; Figure 2D, lower column). Serum PEDF levels were significantly higher in patients with HCC than in patients with non-HCC (Figure 2E). After complete treatment of HCC such as surgical resection or percutaneous radiofrequency ablation, serum PEDF levels were significantly lower than before treatment (Figure 2F).

Effects of PEDF Gene Knockdown on CPT-Induced Apoptosis in HepG2 Cells

Knockdown of the *PEDF* gene was verified by semiquantitative RT-PCR (Figure 3A) and PEDF levels in the culture medium (Figure 3B).

Apoptosis was visualized by FITC-conjugated VAD-FMK, which binds with activated caspase. Laser scanning microscopic images showed a slight increase of apoptosis in *PEDF* gene knockdown HepG2 cells compared with CON and N.CON (Figure 3C, upper column). By treatment with CPT, an apoptotic inducer, marked increase of apoptosis was seen in *PEDF* gene knockdown HepG2 cells compared with CON and N.CON (Figure 3C, lower column).

In addition, apoptosis was quantified by terminal deoxynucleotidyl transferase-mediated dUTP nick-end labeling-based ELISA. *PEDF* gene knockdown increased apoptotic cell numbers in HepG2 cells compared with CON and N.CON (Figure 3D, white bars). By treatment with CPT, a significant increase in apoptotic cell number was seen in knockdown compared with CON and N.CON (Figure 3D, black bars). Similar findings were found in Hep3B and Huh7 cells (Supplemental Figure 1, see *http://ajp.amjpathol.org*).

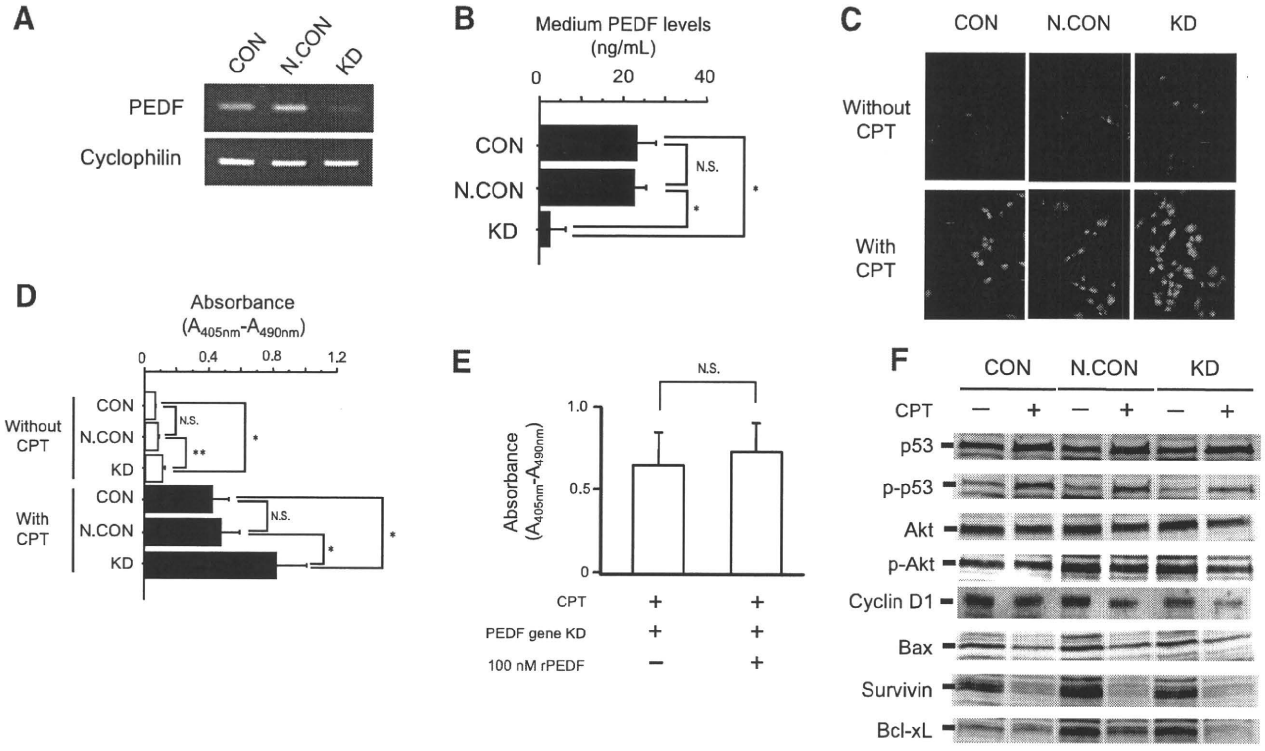

Figure 3. In *PEDF* gene knockdown HepG2 cells, expression of PEDF mRNA (**A**) and medium PEDF levels (**B**) were evaluated by semiquantitative RT-PCR and a competitive ELISA ($n = 4$), respectively. Effects of *PEDF* gene knockdown on CPT-induced apoptosis was examined in HepG2 cells. Apoptosis was visualized by FITC-conjugated VAD-FMK, which binds with activated caspase and green color indicated apoptotic cells (**C**). Apoptosis was quantified by using Cell Death Detection ELISA kits (Roche Applied Science) and increases in absorbance ($A_{405\ nm}$-$A_{490\ nm}$) indicate increased number of apoptotic cells ($n = 4$, **D**). Effects of rPEDF on CPT-induced apoptosis was examined in *PEDF* gene knockdown HepG2 cells. Apoptosis was quantified by using Cell Death Detection ELISA kits (Roche Applied Science) ($n = 4$, **E**). Effects of *PEDF* gene knockdown on cell cycle-related molecules (p53, Akt, and cyclin D1) and apoptosis-related molecules (Bax, survivin, and Bcl-xL) were evaluated by immunoblotting in HepG2 cells (**F**). $^{*}P < 0.01$, $^{**}P < 0.05$.

Effects of Recombinant PEDF on CPT-Induced Apoptosis in PEDF *Gene Knockdown HepG2 Cells*

After addition of recombinant PEDF (rPEDF) (100 nmol/L) into the culture medium, no significant changes were seen in CPT-induced apoptotic cell numbers in *PEDF* gene knockdown HepG2 cells (Figure 3E).

Effects of PEDF *Gene Knockdown on Expression of Cell Cycle- and Apoptosis-Related Molecules in CPT-Treated HepG2 Cells*

Although there was no significant decrease of p53 expression on CPT-treated knockdown cells compared with that in CPT-treated CON and CPT-treated N.CON cells, significant decrease was seen in phospho-p53, Akt, phospho-Akt, and cyclin D1 in CPT-treated knockdown cells compared with those in CPT-treated CON and CPT-treated N.CON cells (Figure 3F and Table 1). Treatment with CPT decreased expression of Bax and survivin in all groups (Figure 3F and Table 1). However, expression of Bcl-xL was markedly decreased in CPT-treated knockdown cells compared with that in CPT-treated CON and CPT-treated N.CON cells (Figure 3F). Decreased expression of Bcl-xL was also found in Hep3B and Huh7 cells (Supplemental Figure 2, see *http://ajp.amjpathol.org*).

Effects of PEDF *Gene Knockdown on Bcl-xL mRNA in HepG2 Cells*

Expression of Bcl-xL mRNA was higher in CPT-treated knockdown cells compared with that in CPT-treated CON and CPT-treated N.CON cells at 6 hours and 12 hours after *PEDF* gene knockdown (Figure 4A).

Effects of MG132 or Bafilomycin A1 on Decreases in Expression of Bcl-xL and Increases in Apoptosis in CPT-Treated PEDF *Gene Knockdown HepG2 Cells*

After treatment with 10 μmol/L of MG132, a proteasomal proteolysis inhibitor, no marked change in expression of Bcl-xL was seen in CPT-treated knockdown cells (Figure 4B). Treatment with 100 nmol/L of bafilomycin A1, a lysosomal proteolysis inhibitor, inhibited decreases in expression of Bcl-xL in CPT-treated knockdown cells (Figure 4B). Treatment with bafilomycin A1, but not MG132, also inhibited an increase of apoptosis in CPT-treated *PEDF* gene knockdown HepG2 cells (Figure 4C).

Table 1. Densitometric Analysis of Expression of Cell Cycle- and Apoptosis-Related Molecules in CPT-Treated HepG2 Cells

Molecule	CON (n = 4)		N.CON (n = 4)		kd (n = 4)	
CPT	−	+	−	+	−	+
P53	223 ± 24	235 ± 19	221 ± 21	232 ± 20	229 ± 21	238 ± 21
p-p53	136 ± 15	193 ± 22	106 ± 17	195 ± 18	101 ± 15	124 ± 26*†
Akt	173 ± 16	169 ± 19	186 ± 16	157 ± 17	182 ± 18	120 ± 25*†
p-Akt	194 ± 18	197 ± 21	242 ± 23	236 ± 22	244 ± 21	160 ± 28*†
cyclin D	215 ± 29	194 ± 31	209 ± 41	164 ± 43	193 ± 37	118 ± 39*†
Bax	132 ± 15	75 ± 11	156 ± 18	85 ± 11	149 ± 12	81 ± 10
Survivin	194 ± 18	56 ± 7	226 ± 21	61 ± 10	210 ± 18	54 ± 9
Bcl-xL	111 ± 13	130 ± 11	215 ± 19	159 ± 15	205 ± 21	87 ± 9‡§

Data presented as mean ± SD.
*$P < 0.05$ compared with CON with CPT.
†$P < 0.05$ compared with N.CON with CPT.
‡$P < 0.01$ compared with CON with CPT.
§$P < 0.01$ compared with N.CON with CPT.

Discussion

In this study, we demonstrated that PEDF was overexpressed not only in human hepatoma cell lines, but also in human HCC tissues. Knockdown of the *PEDF* gene enhanced CPT-induced apoptosis with down-regulation of Bcl-xL expression. Treatment with bafilomycin A1, a lysosomal proteolysis inhibitor, inhibited the CPT-induced decreases in expression of Bcl-xL and increases in apoptotic cell number in *PEDF* gene knockdown HepG2 cells. Thus, PEDF may exert anti-apoptotic effects by inhibiting lysosomal-mediated degradation of Bcl-xL in HepG2 cells.

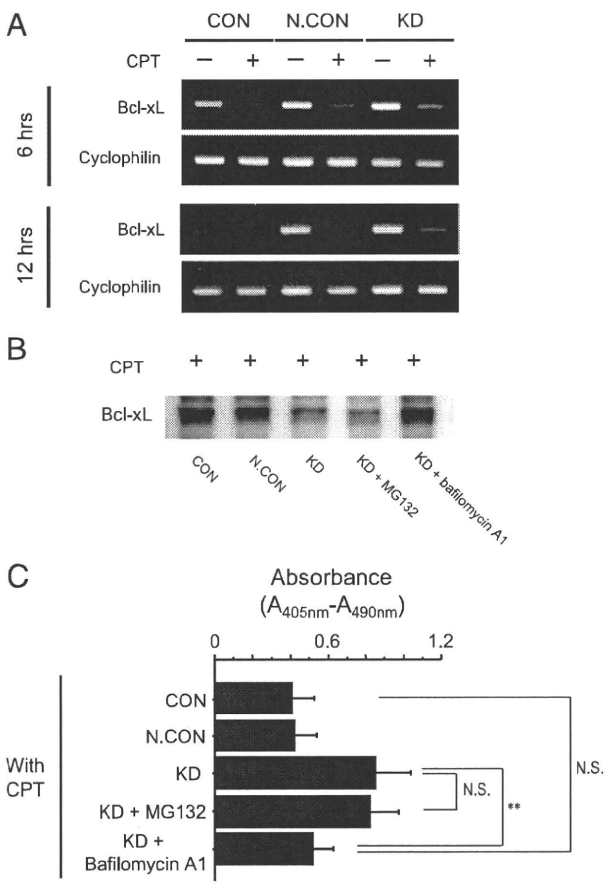

Figure 4. Effects of *PEDF* gene knockdown on Bcl-xL mRNA and cyclophilin mRNA as a control were evaluated by semiquantitative RT-PCR 6 and 12 hours after *PEDF* gene knockdown in CPT-treated HepG2 cells (**A**). In CPT-treated *PEDF* gene knockdown HepG2 cells, effects of 10 μmol/L of MG132 or 100 nmol/L of bafilomycin A1 on expression of Bcl-xL (**B**) and on CPT-induced apoptosis were evaluated by immunoblotting and Cell Death Detection ELISA kits (Roche Applied Science), respectively. Increases in absorbance ($A_{405\ nm}$-$A_{490\ nm}$) indicate increases in number of apoptotic cells (n = 5, **C**). **$P < 0.05$.

Decreased expression of PEDF was reported in various cancers such as prostate,[20] pancreas,[21] breast,[22] and ovarian cancers.[23] PEDF has anti-angiogenic[24] and tumorcidal effects through induction of both apoptosis and differentiation.[25] In fact, treatment with exogenous PEDF has been shown to inhibit neovascularization and proliferation of malignant melanoma *in vivo*.[5] Generally, substitution of PEDF is considered as a novel therapeutic strategy against several cancers. However, there is some controversy about the pathophysiological role of PEDF in cancers because PEDF levels have been increased in some types of cancers.[26,27] Indeed, in this study, we found that PEDF was overexpressed in most of the human hepatoma cell lines and HCC tissues. Although PEDF mRNA was not seen only in HLF cell line, HLF cell line resembles fibroblast in morphology and does not produce alpha-fetoprotein.[28] Thus, HLF cell line shows different characteristics from other hepatoma cell lines and this may be a reason why PEDF mRNA was not seen only in HLF cell line.

More than 99% of PEDF cDNA from HepG2 cells was identical to human PEDF cDNA (data not shown) and therefore, PEDF in HepG2 cells seems to have biological activity. Although treatment with exogenous PEDF is reported as a potential therapeutic strategy for HCC,[29] endogenous expression of PEDF in human HCC has never been investigated and the validity of treatment strategies targeting PEDF has not been confirmed. Expression of PEDF was increased in all six HCC tissues that we examined, although all six HCCs were typical hypervascular tumors. PEDF is known to localize regions of steatosis.[30,31] However, no lipid accumulation was seen in the cytoplasm of HCC and therefore, high expression of PEDF seems to be a character of HCC. Moreover, serum PEDF levels were significantly higher in HCC patients than in non-HCC patients or in HCC patients who had complete treatment. Recently, we, along with others,

have found that adipocytes secrete PEDF and serum PEDF level is associated with metabolic syndrome.[19,32–34] However, in this study, enrolled patients were not obese and there was no significant difference in body mass index between HCC and non-HCC patients (22.5 ± 2.1 vs. 22.3 ± 1.9; not significant). Taken together, PEDF expression levels were increased in HCC as a countersystem against neovascularization. Further, our present results suggest that elevation of PEDF may have other biological effects on HCC, ie, promotion of HCC growth and expansion by suppressing apoptosis.

Because PEDF was expressed in human hepatoma cell lines, knockdown of the *PEDF* gene seemed to be a better strategy for examining the role of PEDF in HCC than overexpression of PEDF or treatment with recombinant PEDF. Knockdown of the *PEDF* gene itself induced apoptosis and the apoptotic effect was enhanced by the co-treatment with CPT, an inducer of apoptosis, in various hepatoma cell lines. These findings indicate that PEDF has a protective role against CPT-induced apoptosis in HepG2 cells. Cao et al[35] reported that PEDF protects cultured retinal neurons against hydrogen peroxide-induced apoptosis. In good accordance with our results, a similar protective role of PEDF against apoptosis has been found in cerebellar granule cells,[7,36–39] retinal pericytes,[8,9] photoreceptor cells,[10,11] and retinal ganglion cells.[40] Addition of rPEDF into the culture medium did not protect CPT-induced apoptosis in *PEDF* gene knockdown HepG2 cells. Although PEDF is a secretory protein,[41,42] these data indicate that PEDF exerted its anti-apoptotic activity through intracellular interaction between PEDF and anti-apoptotic molecules, and not through autocrine or paracrine pathways in HepG2 cells. Precise mechanisms for PEDF-induced protection against apoptosis are unknown. However, several pathways have been suggested. PEDF is known to activate cAMP-responsive element binding protein, nuclear factor κB, extracellular signal-regulated kinases 1/2, and glutathione peroxidase, resulting in protection against apoptosis.[8,38–40] In this study, we found that cell cylcle-related molecules such as phospho-p53, Akt, phospho-Akt, and cyclin D1 were down-regulated by knockdown of the *PEDF* gene in CPT-treated HepG2 cells. These changes were in good accordance with previous reports[43–47] and suggest that cell cycle arrest may enhance CPT-induced apoptosis. In addition to these pathways, we first found that knockdown of the *PEDF* gene down-regulated Bcl-xL, an anti-apoptotic molecule, in CPT-treated HepG2 cells. Thus, PEDF may exert anti-apoptotic effects in HCC through up-regulation of Bcl-xL.

Then, we investigated mechanisms for down-regulation of Bcl-xL by *PEDF* gene knockdown. Expression of Bcl-xL mRNA was decreased in CPT-untreated CON cells at 12 hours after *PEDF* gene knockdown compared with that at 6 hours. Although the reason for down-regulation of Bcl-xL mRNA expression at 12 hours is unclear, the following is a possible reason: HepG2 cells were plated together with siRNA for PEDF. Twenty-four hours later, siRNA for PEDF were removed by replacing them with basal medium containing 1% fetal bovine serum. Fetal bovine serum contains various apoptosis-inducing cytokines including TNF-α. Those apoptosis-inducing cytokines might temporary up-regulate Bcl-xL mRNA expression at 6 hours after *PEDF* gene knockdown and apoptotic stimuli might not last until 12 hours.

Expression of Bcl-xL mRNA was higher in CPT-treated knockdown cells compared with that in CPT-treated CON and CPT-treated N.CON cells at 6 hours and 12 hours after *PEDF* gene knockdown. However, the protein expression of Bcl-xL was lower in CPT-treated knockdown cells. Therefore, we assumed that high expression of Bcl-xL mRNA is a cellular adaptive response against decreased protein expression of Bcl-xL. The ubiquitin-proteasome pathway is a major mechanism for protein degradation. However, treatment with MG132, a proteasomal proteolysis inhibitor, showed no marked changes in expression of Bcl-xL in our study. In concordance with our results, Bcl-xL is not degraded by the ubiquitin-proteasome pathway in ischemic retinal injury.[48] Autophagy is another major mechanism for protein degradation through lysosomal proteolysis.[49] We found that treatment with bafilomycin A1, a lysosomal proteolysis inhibitor, prevented the CPT-induced decrease in expression of Bcl-xL. Treatment with bafilomycin A1 also prevented CPT-induced apoptosis in *PEDF* gene knockdown HepG2 cells. These findings led us to hypothesize that knockdown of the *PEDF* gene causes lysosomal proteolysis-mediated down-regulation of Bcl-xL and subsequent enhancement of CPT-induced apoptosis in HepG2 cells. In other words, PEDF may up-regulate Bcl-xL through inhibition of lysosomal proteolysis in HCC. Supporting our hypothesis, expression of Bcl-xL is known to be increased in human HCC.[50] There are significant correlations between expression of Bcl-xL and disease-free survival, and Bcl-xL is an independent prognostic factor for disease-free survival in patients with HCC.[51]

In the present study, we also examined the expression of PEDF in normal hepatocytes and found that high expression of PEDF was found in cytosol of normal hepatocyte cell line, OUMS-29, but not in non-HCC tissue. Although the reason for this discrepancy is unclear, the following is a possible explanation. PEDF is a secretory protein,[41,42] and cell-matrix interaction is one of the regulatory mechanisms for secretion of PEDF.[52] There is no cell-matrix interaction in culture dish and PEDF was not secreted in the culture medium of OUMS-29. Thus, accumulation of unsecreted PEDF may be a reason for high expression of PEDF in OUMS-29 cells.

A limitation of this study is that a hepatoma xenograft study using nude mice was not conducted to prove the anti-apoptitic property of PEDF. However, continuous and specific down-regulation of *PEDF* gene of hepatoma cell in nude mice is impossible at this point because of following reasons: (1) because effects of knockdown only last 3 days in HepG2 cells (data not shown) and none of *PEDF* knockout hepatoma cells survived for more than 7 days; and (2) PEDF occurs in various organs[53] and therefore, continuous knockdown by injection of siRNA for PEDF affects not only hepatoma cell line, but also various organ functions.

In conclusion, we found increased expression of PEDF in both human hepatoma cell lines and human HCC tissues. Knockdown of the *PEDF* gene enhanced CPT-

induced apoptosis with down-regulation of Bcl-xL expression. Treatment with bafilomycin A1 prevented CPT-induced decreases in expression of Bcl-xL and increases in apoptosis in *PEDF* gene knockdown HepG2 cells. Thus, increased expression of PEDF may exert anti-apoptotic effects in HCC through inhibition of lysosomal degradation of Bcl-xL.

Acknowledgments

We thank Eiichi Hirano and Yumi Ogo for technical assistance.

References

1. Burroughs A, Hochhauser D, Meyer T: Systemic treatment and liver transplantation for hepatocellular carcinoma: two ends of the therapeutic spectrum. Lancet Oncol 2004, 5:409–418
2. Kulik LM, Mulcahy MF, Omary RA, Salem R: Emerging approaches in hepatocellular carcinoma. J Clin Gastroenterol 2007, 41:839–854
3. Tombran-Tink J, Chader GG, Johnson LV: PEDF: a pigment epithelium-derived factor with potent neuronal differentiative activity. Exp Eye Res 1991, 53:411–414
4. Jimenez B, Volpert OV: Mechanistic insights on the inhibition of tumor angiogenesis. J Mol Med 2001, 78:663–672
5. Abe R, Shimizu T, Yamagishi S, Shibaki A, Amano S, Inagaki Y, Watanabe H, Sugawara H, Nakamura H, Takeuchi M, Imaizumi T, Shimizu H: Overexpression of pigment epithelium-derived factor decreases angiogenesis and inhibits the growth of human malignant melanoma cells in vivo. Am J Pathol 2004, 164:1225–1232
6. Garcia M, Fernandez-Garcia NI, Rivas V, Carretero M, Escamez MJ, Gonzalez-Martin A, Medrano EE, Volpert O, Jorcano JL, Jimenez B, Larcher F, Del Rio M: Inhibition of xenografted human melanoma growth and prevention of metastasis development by dual antiangiogenic/antitumor activities of pigment epithelium-derived factor. Cancer Res 2004, 64:5632–5642
7. Araki T, Taniwaki T, Becerra SP, Chader GJ, Schwartz JP: Pigment epithelium-derived factor (PEDF) differentially protects immature but not mature cerebellar granule cells against apoptotic cell death. J Neurosci Res 1998, 53:7–15
8. Amano S, Yamagishi S, Inagaki Y, Nakamura K, Takeuchi M, Inoue H, Imaizumi T: Pigment epithelium-derived factor inhibits oxidative stress-induced apoptosis and dysfunction of cultured retinal pericytes. Microvasc Res 2005, 69:45–55
9. Yamagishi S, Inagaki Y, Amano S, Okamoto T, Takeuchi M, Makita Z: Pigment epithelium-derived factor protects cultured retinal pericytes from advanced glycation end product-induced injury through its antioxidative properties. Biochem Biophys Res Commun 2002, 296:877–882
10. Imai D, Yoneya S, Gehlbach PL, Wei LL, Mori K: Intraocular gene transfer of pigment epithelium-derived factor rescues photoreceptors from light-induced cell death. J Cell Physiol 2005, 202:570–578
11. Miyazaki M, Ikeda Y, Yonemitsu Y, Goto Y, Sakamoto T, Tabata T, Ueda Y, Hasegawa M, Tobimatsu S, Ishibashi T, Sueishi K: Simian lentiviral vector-mediated retinal gene transfer of pigment epithelium-derived factor protects retinal degeneration and electrical defect in Royal College of Surgeons rats. Gene Ther 2003, 10:1503–1511
12. El-Serag HB, Rudolph KL: Hepatocellular carcinoma: epidemiology and molecular carcinogenesis. Gastroenterology 2007, 132:2557–2576
13. Kobayashi N, Miyazaki M, Fukaya K, Inoue Y, Sakaguchi M, Noguchi H, Matsumura T, Watanabe T, Totsugawa T, Tanaka N, Namba M: Treatment of surgically induced acute liver failure with transplantation of highly differentiated immortalized human hepatocytes. Cell Transplant 2000, 9:733–735
14. Kobayashi N, Miyazaki M, Fukaya K, Inoue Y, Sakaguchi M, Uemura T, Noguchi H, Kondo A, Tanaka N, Namba M: Transplantation of highly differentiated immortalized human hepatocytes to treat acute liver failure. Transplantation 2000, 69:202–207
15. Kawaguchi T, Osatomi K, Yamashita H, Kabashima T, Uyeda K: Mechanism for fatty acid "sparing" effect on glucose-induced transcription: regulation of carbohydrate-responsive element-binding protein by AMP-activated protein kinase. J Biol Chem 2002, 277:3829–3835
16. Kawaguchi T, Takenoshita M, Kabashima T, Uyeda K: Glucose and cAMP regulate the L-type pyruvate kinase gene by phosphorylation/dephosphorylation of the carbohydrate response element binding protein. Proc Natl Acad Sci USA 2001, 98:13710–13715
17. Kawaguchi T, Sakisaka S, Sata M, Mori M, Tanikawa K: Different lobular distributions of altered hepatocyte tight junctions in rat models of intrahepatic and extrahepatic cholestasis. Hepatology 1999, 29:205–216
18. Kawaguchi T, Sakisaka S, Mitsuyama K, Harada M, Koga H, Taniguchi E, Sasatomi K, Kimura R, Ueno T, Sawada N, Mori M, Sata M: Cholestasis with altered structure and function of hepatocyte tight junction and decreased expression of canalicular multispecific organic anion transporter in a rat model of colitis. Hepatology 2000, 31:1285–1295
19. Yamagishi S, Adachi H, Abe A, Yashiro T, Enomoto M, Furuki K, Hino A, Jinnouchi Y, Takenaka K, Matsui T, Nakamura K, Imaizumi T: Elevated serum levels of pigment epithelium-derived factor in the metabolic syndrome. J Clin Endocrinol Metab 2006, 91:2447–2450
20. Doll JA, Stellmach VM, Bouck NP, Bergh AR, Lee C, Abramson LP, Cornwell ML, Pins MR, Borensztajn J, Crawford SE: Pigment epithelium-derived factor regulates the vasculature and mass of the prostate and pancreas. Nat Med 2003, 9:774–780
21. Uehara H, Miyamoto M, Kato K, Ebihara Y, Kaneko H, Hashimoto H, Murakami Y, Hase R, Takahashi R, Mega S, Shichinohe T, Kawarada Y, Itoh T, Okushiba S, Kondo S, Katoh H: Expression of pigment epithelium-derived factor decreases liver metastasis and correlates with favorable prognosis for patients with ductal pancreatic adenocarcinoma. Cancer Res 2004, 64:3533–3537
22. Cai J, Parr C, Watkins G, Jiang WG, Boulton M: Decreased pigment epithelium-derived factor expression in human breast cancer progression. Clin Cancer Res 2006, 12:3510–3517
23. Cheung LW, Au SC, Cheung AN, Ngan HY, Tombran-Tink J, Auersperg N, Wong AS: Pigment epithelium-derived factor is estrogen sensitive and inhibits the growth of human ovarian cancer and ovarian surface epithelial cells. Endocrinology 2006, 147:4179–4191
24. Dawson DW, Volpert OV, Gillis P, Crawford SE, Xu H, Benedict W, Bouck NP: Pigment epithelium-derived factor: a potent inhibitor of angiogenesis. Science 1999, 285:245–248
25. Ek ET, Dass CR, Choong PF: PEDF: a potential molecular therapeutic target with multiple anti-cancer activities. Trends Mol Med 2006, 12:497–502
26. Crawford SE, Stellmach V, Ranalli M, Huang X, Huang L, Volpert O, De Vries GH, Abramson LP, Bouck N: Pigment epithelium-derived factor (PEDF) in neuroblastoma: a multifunctional mediator of Schwann cell antitumor activity. J Cell Sci 2001, 114:4421–4428
27. Tsuru M, Arima N, Toyozumi Y, Kato S: Pigment epithelium-derived factor as a new diagnostic marker for melanocytic tumors. Kurume Med J 2005, 52:81–87
28. Dor I, Namba M, Sato J: Establishment and some biological characteristics of human hepatoma cell lines. Gann 1975, 66:385–392
29. Matsumoto K, Ishikawa H, Nishimura D, Hamasaki K, Nakao K, Eguchi K: Antiangiogenic property of pigment epithelium-derived factor in hepatocellular carcinoma. Hepatology 2004, 40:252–259
30. Chung C, Doll JA, Gattu AK, Shugrue C, Cornwell M, Fitchev P, Crawford SE: Anti-angiogenic pigment epithelium-derived factor regulates hepatocyte triglyceride content through adipose triglyceride lipase (ATGL). J Hepatol 2008, 48:471–478
31. Chung C, Shugrue C, Nagar A, Doll JA, Cornwell M, Gattu A, Kolodecik T, Pandol SJ, Gorelick F: Ethanol exposure depletes hepatic pigment epithelium-derived factor, a novel lipid regulator. Gastroenterology 2009, 136:331–340
32. Kratchmarova I, Kalume DE, Blagoev B, Scherer PE, Podtelejnikov AV, Molina H, Bickel PE, Andersen JS, Fernandez MM, Bunkenborg J, Roepstorff P, Kristiansen K, Lodish HF, Mann M, Pandey A: A proteomic approach for identification of secreted proteins during the differentiation of 3T3-L1 preadipocytes to adipocytes. Mol Cell Proteomics 2002, 1:213–222
33. Nakamura K, Yamagishi S, Adachi H, Kurita-Nakamura Y, Matsui T, Inoue H: Serum levels of pigment epithelium-derived factor (PEDF) are positively associated with visceral adiposity in Japanese patients with type 2 diabetes. Diabetes Metab Res Rev 2009, 25:52–56
34. Nakamura K, Yamagishi SI, Adachi H, Matsui T, Kurita Y, Imaizumi T:

Serum levels of pigment epithelium-derived factor (PEDF) are an independent determinant of insulin resistance in patients with essential hypertension. Int J Cardiol 2008 doi: 10.1016/j.ijcard.2008.11.169
35. Cao W, Tombran-Tink J, Chen W, Mrazek D, Elias R, McGinnis JF: Pigment epithelium-derived factor protects cultured retinal neurons against hydrogen peroxide-induced cell death. J Neurosci Res 1999, 57:789–800
36. Taniwaki T, Becerra SP, Chader GJ, Schwartz JP: Pigment epithelium-derived factor is a survival factor for cerebellar granule cells in culture. J Neurochem 1995, 64:2509–2517
37. Taniwaki T, Hirashima N, Becerra SP, Chader GJ, Etcheberrigaray R, Schwartz JP: Pigment epithelium-derived factor protects cultured cerebellar granule cells against glutamate-induced neurotoxicity. J Neurochem 1997, 68:26–32
38. Yabe T, Kanemitsu K, Sanagi T, Schwartz JP, Yamada H: Pigment epithelium-derived factor induces pro-survival genes through cyclic AMP-responsive element binding protein and nuclear factor kappa B activation in rat cultured cerebellar granule cells: implication for its neuroprotective effect. Neuroscience 2005, 133:691–700
39. Yabe T, Wilson D, Schwartz JP: NFkappaB activation is required for the neuroprotective effects of pigment epithelium-derived factor (PEDF) on cerebellar granule neurons. J Biol Chem 2001, 276: 43313–43319
40. Pang IH, Zeng H, Fleenor DL, Clark AF: Pigment epithelium-derived factor protects retinal ganglion cells. BMC Neurosci 2007, 8:11
41. Tombran-Tink J, Barnstable CJ: PEDF: a multifaceted neurotrophic factor. Nat Rev Neurosci 2003, 4:628–636
42. Tombran-Tink J, Shivaram SM, Chader GJ, Johnson LV, Bok D: Expression, secretion, and age-related downregulation of pigment epithelium-derived factor, a serpin with neurotrophic activity. J Neurosci 1995, 15:4992–5003
43. Ho TC, Chen SL, Yang YC, Liao CL, Cheng HC, Tsao YP: PEDF induces p53-mediated apoptosis through PPAR gamma signaling in human umbilical vein endothelial cells. Cardiovasc Res 2007, 76:213–223
44. Nakamura K, Yamagishi S, Matsui T, Yoshida T, Takenaka K, Jinnouchi Y, Yoshida Y, Ueda S, Adachi H, Imaizumi T: Pigment epithelium-derived factor inhibits neointimal hyperplasia after vascular injury by blocking NADPH oxidase-mediated reactive oxygen species generation. Am J Pathol 2007, 170:2159–2170
45. Sasaki Y, Naishiro Y, Oshima Y, Imai K, Nakamura Y, Tokino T: Identification of pigment epithelium-derived factor as a direct target of the p53 family member genes. Oncogene 2005, 24:5131–5136
46. Tombran-Tink J: The neuroprotective and angiogenesis inhibitory serpin. PEDF: new insights into phylogeny, function, and signaling. Front Biosci 2005, 10:2131–2149
47. Zhang T, Guan M, Xu C, Chen Y, Lu Y: Pigment epithelium-derived factor inhibits glioma cell growth in vitro and in vivo. Life Sci 2007, 81:1256–1263
48. Harada T, Harada C, Wang YL, Osaka H, Amanai K, Tanaka K, Takizawa S, Setsuie R, Sakurai M, Sato Y, Noda M, Wada K: Role of ubiquitin carboxy terminal hydrolase-L1 in neural cell apoptosis induced by ischemic retinal injury in vivo. Am J Pathol 2004, 164:59–64
49. Kiffin R, Christian C, Knecht E, Cuervo AM: Activation of chaperone-mediated autophagy during oxidative stress. Mol Biol Cell 2004, 15:4829–4840
50. Takehara T, Liu X, Fujimoto J, Friedman SL, Takahashi H: Expression and role of Bcl-xL in human hepatocellular carcinomas. Hepatology 2001, 34:55–61
51. Watanabe J, Kushihata F, Honda K, Sugita A, Tateishi N, Mominoki K, Matsuda S, Kobayashi N: Prognostic significance of Bcl-xL in human hepatocellular carcinoma. Surgery 2004, 135:604–612
52. Ma DH, Yao JY, Yeh LK, Liang ST, See LC, Chen HT, Lin KY, Liang CC, Lin KK, Chen JK: In vitro antiangiogenic activity in ex vivo expanded human limbocorneal epithelial cells cultivated on human amniotic membrane. Invest Ophthalmol Vis Sci 2004, 45:2586–2595
53. Singh VK, Chader GJ, Rodriguez IR: Structural and comparative analysis of the mouse gene for pigment epithelium-derived factor (PEDF). Mol Vis 1998, 4:7

European Journal of Radiology 75 (2010) e32–e37

Contents lists available at ScienceDirect

European Journal of Radiology

journal homepage: www.elsevier.com/locate/ejrad

Pre-treatment hemodynamic features involved with long-term survival of cirrhotic patients after embolization of gastric fundal varices

Hitoshi Maruyama*, Hidehiro Okugawa, Satoshi Kobayashi, Hiroaki Yoshizumi, Osamu Yokosuka

Department of Medicine and Clinical Oncology, Chiba University Graduate School of Medicine, 1-8-1, Inohana, Chuou-ku, Chiba, 260-8670, Japan

ARTICLE INFO

Article history:
Received 7 September 2009
Received in revised form 30 October 2009
Accepted 4 November 2009

Keywords:
Gastric varices
Doppler ultrasound
Portal hypertension
Balloon-occluded retrograde transvenous obliteration (B-RTO)

ABSTRACT

Purpose: To clarify the pre-treatment hemodynamic features involved in the long-term survival of cirrhotic patients with gastric fundal varices (FV) after balloon-occluded retrograde transvenous obliteration (B-RTO).

Materials and methods: Eighty-one cirrhotic patients with medium- or large-grade FV treated by B-RTO were enrolled in this retrospective study. Pre-treatment flow volume ratio between gastric vein and portal trunk (GP-R) was obtained by Doppler ultrasound.

Results: The cumulative survival rate was 90% at 1 year, 74.8% at 3 years, 57.2% at 5 years, and 45.8% at 7 years without recurrence in a median period of 1148.5 days The survival was poorer in patients with HCC (47% at 3 years, 9.4% at 5 years, $p < 0.0001$) than without (89.2% at 3 years, 81.9% at 5 years, 67.5% at 7 years), in patients with Child B/C (57.7% at 3 years, 42.1% at 5 years, 28.1% at 7 years, $p = 0.0016$) than with Child A (91.8% at 3 years, 71.5% at 5 years, 62.1% at 7 years), and in patients with GP-R $\geq$ 1.0 (58.9% at 3 years, $p = 0.0485$) than with GP-R < 1.0 (76.3% at 3 years, 62% at 5 years, 49.6% at 7 years). Multivariate analysis identified the presence of HCC (hazard ratio, 12.486; 95% CI, 4.08–38.216; $p < 0.0001$), Child B/C (hazard ratio, 3.41; 95% CI, 1.594–7.15; $p = 0.0051$) and GP-R $\geq$ 1.0 (hazard ratio, 2.701; 95% CI, 1.07–6.15; $p = 0.0221$) as independent factors for poor prognosis.

Conclusion: GP-R $\geq$ 1.0 on Doppler ultrasound before B-RTO may be a predictive indicator for poor prognosis in cirrhotic patients with FV after B-RTO, in addition to the presence of HCC and severe liver damage.

1. Introduction

Portal hypertension causes gastroesophageal varices, which present a certain bleeding risk [1]. Although lower bleeding rates of gastric varices compared to esophageal varices (EV) have been reported, gastric variceal bleeding sometimes results in serious consequences during the clinical course [2,3]. As variceal bleeding is still one of the major causes of mortality in cirrhotic patients, certain treatment methods using endoscopy, surgery or interventional techniques have been introduced and applied for gastric varices [4,5].

Balloon-occluded retrograde transvenous obliteration (B-RTO) provides an efficient therapeutic effect for gastric fundal varices (FV) with less recurrence [6–8]. Previous reports have shown satisfactory prognosis after B-RTO, with 3- and 5-year survival rates over 70% and 50%, respectively, and hepatocellular carcinoma (HCC) and/or liver function were reported to be prognostic factors associated with survival after the treatment [9–11].

As B-RTO embolizes large collateral vessels, portal hemodynamic changes may occur in the manner of an opposite effect to a decompressive treatment like transjugular intrahepatic portosystemic shunt. In fact, Akahane et al. reported a significant increase in portal venous pressure (PVP) as a logical consequence after B-RTO, with an increase in portal blood flow [12]. Although portal hemodynamics before B-RTO might predict the clinical course after B-RTO, the relationship between pre-treatment hemodynamics and post-treatment prognosis has not been fully investigated. The aim of this study was to clarify the pre-treatment clinical parameters including hemodynamic conditions involved in the long-term survival of cirrhotic patients with FV after B-RTO.

2. Patients and methods

2.1. Patients

Between March 1998 and August 2007, 98 cirrhotic patients underwent B-RTO for medium- or large-grade FV in Chiba University Hospital. The application criteria for B-RTO in our department

* Corresponding author. Tel.: +81 43 2262083; fax: +81 43 2262088.
E-mail addresses: maru-cib@umin.ac.jp (H. Maruyama), hideun@yahoo.co.jp (H. Okugawa), kobakobakopa@yahoo.co.jp (S. Kobayashi), yossih04@yahoo.co.jp (H. Yoshizumi), yokosukao@faculty.chiba-u.jp (O. Yokosuka).

0720-048X/$ – see front matter © 2009 Elsevier Ireland Ltd. All rights reserved.
doi:10.1016/j.ejrad.2009.11.007

were as follows: (i) patients with medium- or large-grade FV on endoscopy, (ii) patients with a bleeding history from FV (secondary prophylaxis), (iii) Child's A or B grade patients with hopeful prophylaxis treatment for FV (primary prophylaxis), (iv) patients with gastrorenal shunt and/or inferior phrenic vein for the drainage route of FV on ultrasound (US), computed tomography (CT) or percutaneous transhepatic portography images. Among the 98 patients, eligible subjects for this study were selected according to the following criteria: (i) patients with FV completely embolized on contrast-enhanced CT after B-RTO, (ii) patients followed up on an outpatient basis for 1 year or more, (iii) patients received a medical check-up with blood tests at least twice a year, and had US examination and endoscopy at least once a year. Complete embolization of FV was obtained in 94 of the 98 patients, and the clinical course of 13 patients became unknown within 1 year because they stopped visiting to the hospital. Therefore, data on 81 cirrhotic patients (age: 63.5 ± 9.4, 42–80 years; male 47, female 34) with medium- or large-grade FV treated by B-RTO were analyzed in this retrospective study. The cause of cirrhosis was viral in 57 patients (HCV 49, HBV 8), alcohol abuse in 12, primary biliary cirrhosis in two, autoimmune hepatitis in one, and cryptogenic in nine. The severity of liver function (Child-Pugh score) was A in 39, B in 39, and C in three, and laboratory findings just before B-RTO were as follows: total bilirubin 1.5 ± 1.7 (0.2–15.4 mg/dl), serum albumin 3.2 ± 0.5 (2–4.5 g/dl), prothrombin time 67.6 ± 14.7 (18–107%).

At the time of B-RTO, 18 patients had concomitant HCC, of which the number of nodules was one in seven patients, two in four patients, three in three patients and more than three in four patients. The diameter of the nodules ranged 10–45 mm (mean 24.8 ± 12.3). One patient had portal vein tumor thrombosis in the portal trunk, and none had distant metastasis. They received treatments for HCC after B-RTO — surgical treatment in one, percutaneous ethanol injection (PEI) in three, transcatheter arterial chemoembolization (TACE) in eight, and TACE followed by PEI in six. Meanwhile, nine patients had a treatment history of HCC, which was controlled by non-surgical treatments in eight (PEI in four, radiofrequency ablation in three, TACE in one) and surgical treatment in one. Therefore, 54 of the 81 patients had neither concomitant HCC nor treatment history of HCC.

Informed written consent was obtained from all patients, and the investigation was carried out in accordance with the Helsinki Declaration. This retrospective study was judged as having an appropriate design for publication by the ethics committee of our hospital.

2.2. Endoscopy

Endoscopic findings of FV and EV were classified according to the General Rules for Recording Endoscopic Findings set by the Japan Research Society for Portal Hypertension [13]; F1 (straight), F2 (winding), and F3 (nodule-beaded), corresponding to the grades of small, medium and large, respectively. The grades of FV were F2 in 42 and F3 in 39; 37 of the FV patients were accompanied by EV, F1 in 22 and F2 in 15. According the FV classification by Sarin et al, there were 44 patients with IGV1 and 37 patients with GOV2 [1]. Forty-four of the 81 FV patients were bleeders, 32 confirmed by endoscopy and 12 by clinical symptoms of hematemesis or melena; the other 37 were non-bleeders with no history of hematemesis or melena. Twenty-four of the 44 bleeder patients underwent emergent endoscopic treatment for hemostasis of FV bleeding, sclerotherapy in 20, band ligation in two, and clipping in two. Prophylactic treatment (band ligation followed by sclerotherapy with absolute ethanol) for EV was done in two patients with medium-grade EV, one before B-RTO and one after B-RTO. All endoscopic procedures were performed by H.M. and S.K. Follow-up endoscopy was performed approximately every 6–12 months after B-RTO, and aggravation of EV was defined when the grade of EV worsened.

2.3. US examination

The US system used in the present study was SSA-270A, SSA-390A and SSA-770A (Toshiba, Tokyo, Japan) with a 3.75-MHz convex or sector probe. Mean flow volume (ml/min) of the portal trunk and gastric vein before B-RTO was measured by pulsed Doppler method in all patients under a fasting state of over 6 h, with the sampling width corresponding to the maximum diameter of the vessel and at an angle less than 60° between the US beam and the vessel. Demonstration of gastric vein was done as previously reported [14,15], using a middle longitudinal or oblique scan for the left gastric vein (LGV), and a left intercostal scan for the short gastric vein (SGV). In cases with multiple gastric veins, that with the highest flow volume showing hepatofugal flow direction was chosen for Doppler measurement result. All US examinations were performed by H.M., and 22 of the 81 patients also received second Doppler measurements by H.O. or H.Y. The US operators had more than 8 years of experience with US. Blood flow measurement was performed two or more times in each patient, and the average value was obtained for each vessel. With the use of these data, the flow volume ratio of gastric vein to portal trunk (GP-R) was calculated in each patient. When the blood flow in the portal trunk had to and fro appearance, the data were not used for GP-R. The results obtained by second US examination were used only for the measurement of inter-observer variability.

2.4. B-RTO

The application of B-RTO represented secondary prophylaxis for 44 bleeders and primary prophylaxis for 37 non-bleeders. B-RTO was conducted by H.M., H.O., S.K. and H.Y. by standard technique using a balloon catheter (Selecon balloon catheter; 5-French, 9 mm, 13 mm; 6-French, 20 mm, Clinical Supply, Gifu, Japan) as previously reported [6–8]. The outflow route of FV for balloon catheter insertion was the gastrorenal shunt in 77 patients, inferior phrenic vein in one, and both in three. The sclerosing agent which contained equal amounts of 10% ethanolamine oleate (Oldamin, Mochida Pharmaceutical, Tokyo, Japan) and iopamidole 300 (Iopamiron 300; Schering, Osaka, Japan) was administered via the catheter to fill both the gastric varices and inflow vessels under balloon occlusion from 1 h to overnight. Haptoglobin (200 ml; Midori Jyuji, Osaka, Japan) was administered continuously to prevent hemolysis. The embolization effect in FV was evaluated on contrast-enhanced CT within 1 week after B-RTO in all patients.

2.5. Statistical analysis

All results were expressed as mean ± standard deviation (SD) or percentage. The survival time of the patients was based on the date of death, liver transplantation or final date confirmed to be alive during the study period. The Kaplan–Meier method was used to calculate survival probabilities for each clinical background, and the difference was compared with log-rank test. The analysis for survival was done by Cox's proportional hazards models with univariate and multivariate using step-wise method. The results were reported as hazard ratios with 95% confidence intervals (CI). Inter-observer variability was calculated with coefficient of variation, calculated by dividing the standard deviation by mean and multiplying by 100. p-Value less than 0.05 was considered statistically significant in all analyses. Statistical analysis was performed using the Dr. SPSS package (version 11.0J for Windows; SPSS Inc., Chicago, IL, USA).

3. Results

3.1. Clinical course, prognosis and causes of death after B-RTO

The median follow-up period after B-RTO was 1148.5 days, the mean being 1292.6 ± 930.7, 60–3645 days. Although there were only minor short-term complications, fever (over 37.5 °C, 56%), hemoglobinuria (74%) and pain (38%), all cases recovered within 3 days. Aggravation of EV was found in 57 patients (72.2%) and four patients (5.1%) bled from EV after B-RTO among 79 patients who did not receive prophylactic treatment for EV. Neither recurrence nor rebleeding of FV was encountered in this study (Fig. 1). The cumulative overall survival rate was 90% at 1 year, 74.8% at 3 years, 57.2% at 5 years, and 45.8% at 7 years. Thirty-one patients (38.3%) died, with the causes of death being HCC in 13, hepatic failure in 13, other malignancies in three, and sudden death of unknown cause in two. The 3 Child's C grade bleeders were anxious to receive B-RTO, and their survival was 60, 214 and 455 days, respectively, with the cause of death being hepatic failure, metastatic liver tumor from breast cancer and HCC rupture.

3.2. Portal hemodynamics on Doppler US before B-RTO

Blood flow direction in the portal trunk was hepatopetal in 73 patients, to and fro in five patients, and the other three had poor visualization. The main gastric vein was the short gastric vein in 53 (65.4%) and the left gastric vein in 19 (23.5%), showing hepatofugal flow direction on sonograms, and US could not demonstrate gastric veins in nine patients (11.1%). The presence of the gastric veins in 72 patients was confirmed on retrograde

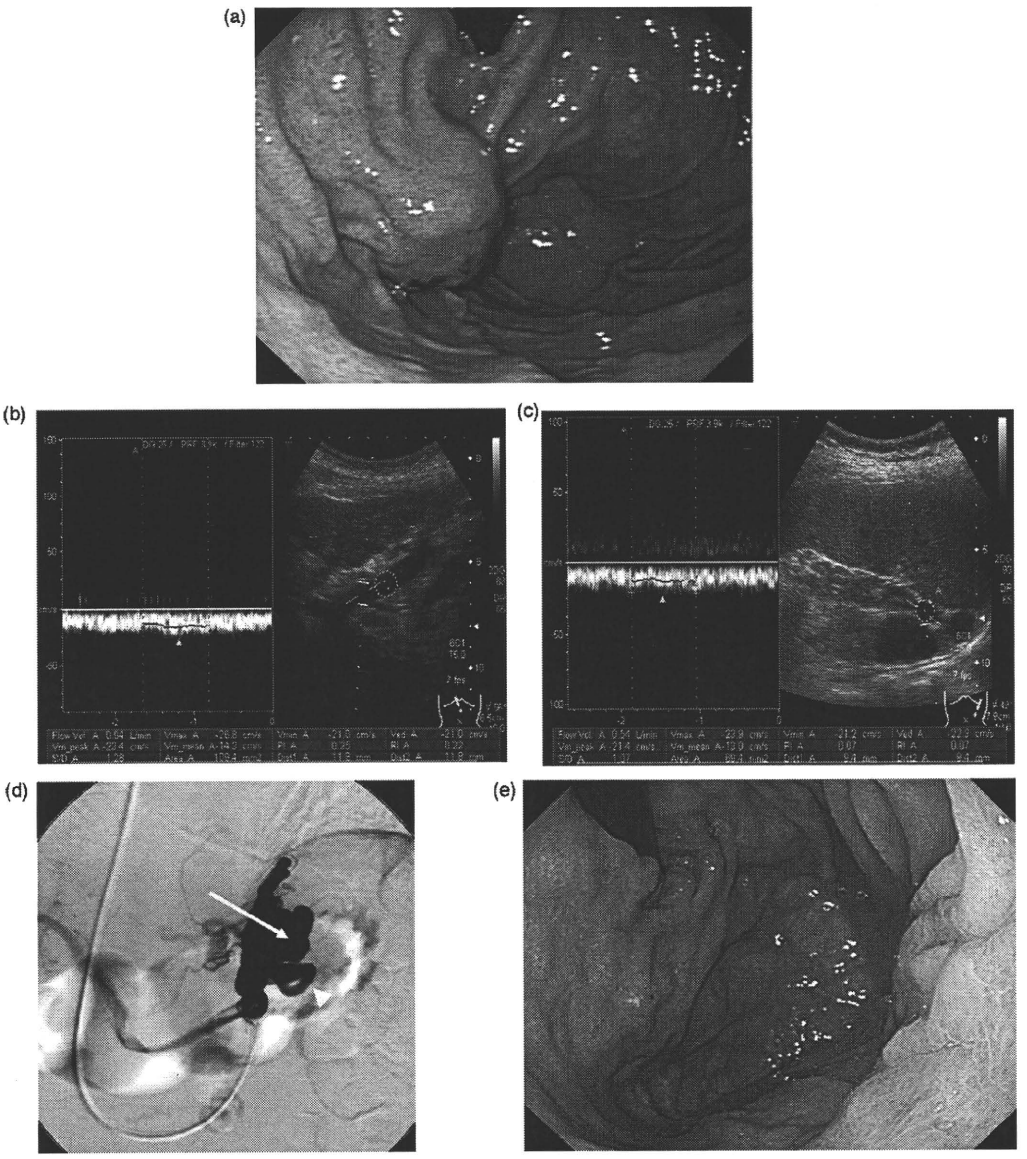

Fig. 1. 61-year-old female, cirrhotic patient (HCV positive), non-bleeder (prophylactic treatment). (a) Endoscopic finding before B-RTO. Large-grade FV was demonstrated at the fundus of the stomach. (b) Doppler US finding. The mean flow volume of the portal trunk was 940 ml/min before B-RTO. (c) Doppler US finding. Doppler US showed development of the short gastric vein with a mean flow volume of 540 ml/min before B-RTO. GP-R of this patient was 0.57 (540/940). (d) Retrograde venography at the time of B-RTO. FV (arrow) and short gastric vein (arrowhead) were demonstrated on this image. (e) Endoscopic finding after B-RTO. FV disappeared completely after B-RTO, and this case was alive 690 days after B-RTO.

Table 1
Univariate analysis of potential risk factors for survival in patients with gastric fundal varices.

	HR[a]	95% CI[b]	*p*-Value
Gender (F)	0.828	0.389–1.760	0.623
Age	1.007	0.964–1.052	0.7395
HCC[c]	8.907	3.606–22.002	<0.0001
Application[d]	0.698	0.332–1.468	0.3436
Grade of FV[e]	1.334	0.628–2.836	0.4533
EIS	0.719	0.324–1.594	0.4164
EV (before)	0.697	0.329–1.476	0.3461
EV (after)	0.515	0.301–1.449	0.2952
Child B, C	3.476	1.524–7.930	0.0031
PV[f]	0.999	0.998–1.0	1.747
Gastric vein[f]	1.001	0.999–1.002	0.3974
GP-R[g]	2.794	1.064–7.812	0.0487

EV (before): presence of esophageal varices before B-RTO. EV (after): aggravated or bleeding esophageal varices after B-RTO.
[a] Hazard ratio.
[b] Confidence interval.
[c] Concomitant or treatment history.
[d] Secondary prophylaxis.
[e] Medium-grade FV.
[f] Mean flow volume.
[g] Flow volume ratio of gastric vein to portal trunk ≥1.0.

venograms, though 10 of the 53 gastric veins judged to be SGV by US appeared as posterior gastric veins by retrograde venography. The mean flow volume in the portal trunk with hepatopetal flow was 669.8 ± 344.2 ml/min (n = 73) and that in the gastric vein was 326.5 ± 365.3 ml/min (n = 72). Average GP-R was 0.48 ± 0.58 (n = 70), and 11 patients (15.7%) had GP-R ≥ 1.0. The inter-observer variability was 10.7 ± 5.4% for Doppler measurement results.

3.3. Survival rate and clinical background

Univariate analysis showed that concomitant/history of HCC (hazard ratio, 8.907; 95% CI, 3.606–22.002; $p < 0.0001$), liver function of Child B/C (hazard ratio, 3.476; 95% CI, 1.524–7.930; $p = 0.0031$) and GP-R ≥ 1.0 (hazard ratio 2.794; 95% CI, 1.064–7.812; $p = 0.0487$) were significant factors for poor prognosis (Table 1). Concomitant HCC (hazard ratio, 11.822; 95% CI, 4.15–33.69; $p < 0.0001$) and history of HCC (hazard ratio, 6.951; 95% CI, 2.41–20.02; $p = 0.0003$) were also significant factors for poor prognosis, and the cumulative survival rate in Child A cases with neither concomitant HCC nor history of HCC was 92.3% at 5 years and 83.9% at 7 years. The cumulative survival rate was poorer in patients with concomitant HCC or a history of HCC (47% at 3 years, 9.4% at 5 years, $p < 0.0001$) than in patients without (89.2% at 3 years, 81.9% at 5 years, 67.5% at 7 years), in patients with Child B or C (57.7% at 3 years, 42.1% at 5 years, 28.1% at 7 years, $p = 0.0016$) than patients with Child A (91.8% at 3 years, 71.5% at 5 years, 62.1% at 7 years), and in patients with GP-R ≥ 1.0 (58.9% at 3 years, $p = 0.0485$) than in patients with GP-R < 1.0 (76.3% at 3 years, 62% at 5 years, 49.6% at 7 years; Fig. 2). Multivariate analysis identified the presence of HCC (hazard ratio, 12.486; 95% CI, 4.08–38.216; $p < 0.0001$, liver function of Child B or C (hazard ratio, 3.41; 95% CI, 1.594–7.15; $p = 0.0051$), and GP-R ≥ 1.0 (hazard ratio, 2.701; 95% CI, 1.07–6.15; $p = 0.0221$) as independent factors for poor prognosis (Table 2).

4. Discussion

The therapeutic effects of B-RTO for FV could be concisely summarized as an efficient embolization effect and less recurrence [7,8]. All 81 patients treated by B-RTO in our study remained free of FV recurrence during the clinical course of 1292.6 ± 930.7 (60–3645) days, showing a satisfactory therapeutic effect similar to some previous reports [9–11].

Table 2
Multivariate analysis of potential risk factors for survival in patients with gastric fundal varices.

	HR[a]	95% CI[b]	*p*-Value
HCC[c]	12.5	4.08–38.22	<0.0001
Child B, C	3.41	1.594–7.15	0.0051
GP-R[d]	2.701	1.07–6.15	0.02

[a] Hazard ratio.
[b] Confidence interval.
[c] Concomitant or treatment history..
[d] Flow volume ratio of gastric vein to portal trunk ≥1.0.

As for the longitudinal clinical course aspect, the survival rate after B-RTO of our study was almost the same as that of the previous reports — 76% at 3 years and 54% at 5 years by Ninoi et al. [9], 68% at 5 years by Hiraga et al. [10], and 76% at 3 years, 61% at 5 years and 47% at 8 years by Chikamori et al. [11], and the backgrounds of their patients were also quite similar. These results may suggest that the successful B-RTO procedure provides a stable long-term therapeutic effect irrespective of the facility. Meanwhile, inevitable concern may arise regarding the relationship between the load on portal hemodynamics after B-RTO and survival, because B-RTO embolizes large collateral vessels with a large amount of blood flow [16,17]. To assess the severity of the portal hemodynamics on FV, we proposed here the ratio of mean blood flow volume between gastric vein and portal trunk (GP-R) as an important predictive factor for poor prognosis of cirrhotic patients with FV after B-RTO, though approximately 10% inter-observer variability should be taken into account. In this regard, however, it should be emphasized that this result does not necessarily limit the application of B-RTO for FV, because only 15% of the patients had GP-R equal to or more than 1.0, and patients with GP-R less than 1.0 showed acceptable long-term survival: 76.3% at 3 years, 62% at 5 years, and 49.6% at 7 years. In contrast, embolization of FV in patients with GP-R equal to or more than 1.0 might result in excessive congestion in the portal venous system. In fact, Chikamori et al. reported that application of partial splenic embolization (PSE) was effective for preventing the hemodynamic congestion after B-RTO [18]. However, as PSE is invasive and requires additional radiation exposure, the use of Doppler US before B-RTO might be effective for selecting appropriate candidates that require PSE.

Doppler US could demonstrate neither portal trunk in three patients (3.7%) nor gastric vein in nine patients (11.1%) in our study. As it is reported that microbubble contrast agents have improved the blood flow detection by US [19], application of contrast-enhanced US might increase the detection rate of portal vein and gastric veins. However, presence of microbubble in the vessel influences the measurement results of flow velocity and/or flow volume by pulsed Doppler method [20]. This dilemma remains to be solved in the future.

Significant non-hemodynamic factors regarding prognosis after B-RTO, HCC and liver function reserve were noted in our study, while the cumulative survival rate in Child A cases with neither concomitant HCC nor history of HCC was quite good; 92.3% at 5 years and 83.9% at 7 years. In particular, HCC was the most influential factor, similar to that of previous reports, which showed survival rates at 1, 3 and 5 years after B-RTO to be 83%, 60%, and 18% by Ninoi et al. [9], and 100%, 64%, and 21% by Chikamori et al. [11] in HCC patients. The results of those two reports were somewhat better than ours, the reason possibly related to a different progression of HCC. Concerning this point, the definition of the patients with HCC differed between their studies and ours, as we adopted patients with concomitant HCC or a history of HCC in this study. Based on this, however, we had the interesting result that the treatment history of HCC as well as concomitant HCC was a significant factor for poor prognosis after B-RTO.

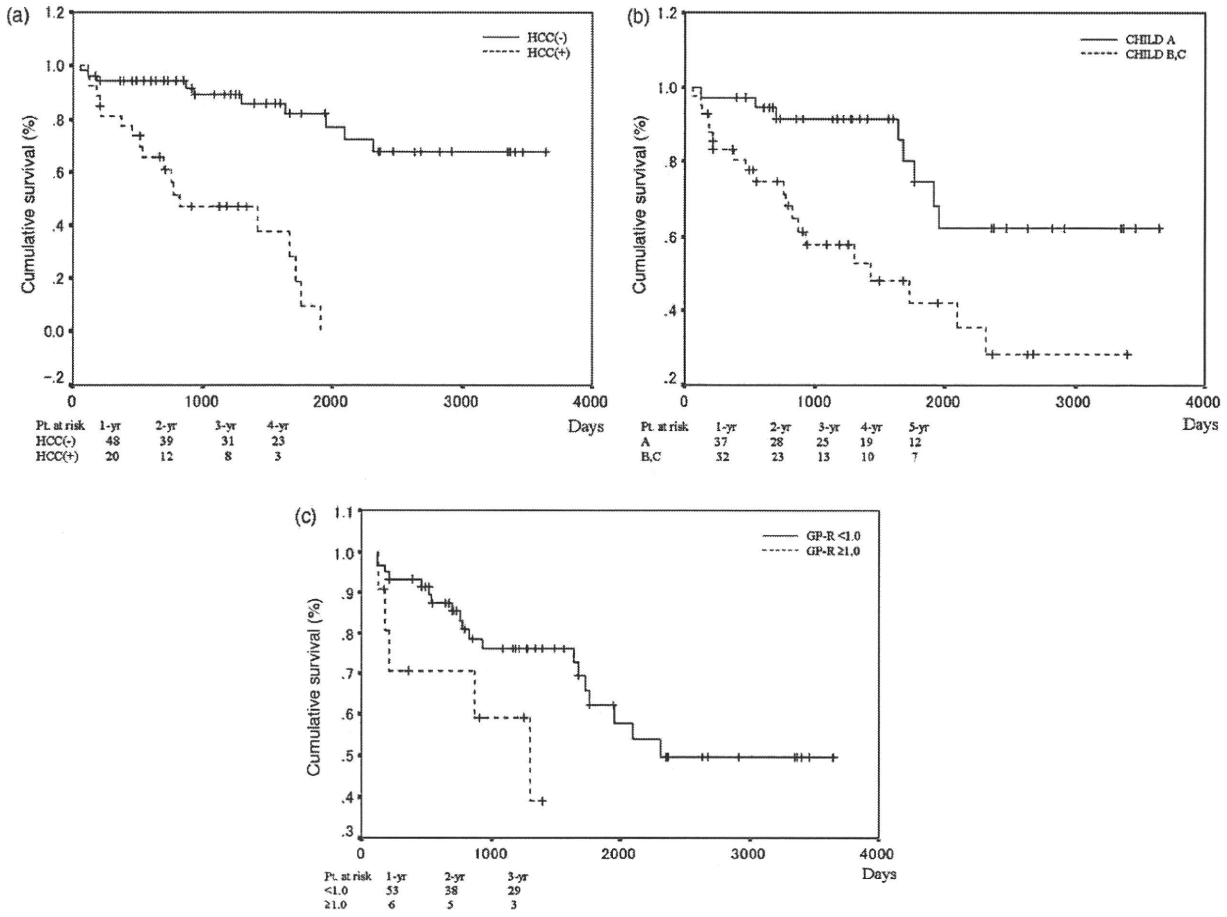

Fig. 2. Cumulative survival rate of cirrhotic patients with FV after B-RTO. (a) Cumulative survival rate was poorer in patients with concomitant HCC or history of HCC (47% at 3 years, 9.4% at 5 years, $p < 0.0001$) than in patients without (89.2% at 3 years, 81.9% at 5 years, 67.5% at 7 years). (b) Cumulative survival rate was poorer in patients with Child B or C (57.7% at 3 years, 42.1% at 5 years, 28.1% at 7 years, $p = 0.0016$) than in patients with Child A (91.8% at 3 years, 71.5% at 5 years, 62.1% at 7 years). (c) Cumulative survival rate was poorer in patients with GP-R $\geq$ 1.0 (58.9% at 3 years, $p = 0.0485$) than in patients with GP-R < 1.0 (76.3% at 3 years, 62% at 5 years, 49.6% at 7 years).

This needs to be considered in the management of patients after B-RTO.

All B-RTO procedures were safely performed in our study, in spite of some minor short-term complications. However, aggravation of EV was found over 70% patients and 5.1% bled from EV after B-RTO probably due to the increase of portal venous pressure after B-RTO. Although aggravated or bleeding EV was not a significant factor for the prognosis in our study, this may be a careful adverse event of this treatment. Application and optimal timing of prophylactic treatment for EV need to be standardized in the B-RTO cases.

Endoscopic injection therapy such as cyanoacrylate or alcohol injection is effective for attaining hemostasis in bleeding FV. However, such treatment alone does not always provide sufficient long-term protection against FV bleeding, and previous reports have shown a cumulative rebleeding rate from 18% to 33% per year after cyanoacrylate injection [21,22]. Although band ligation is another method for treating bleeding FV and is easy to perform [23,24], the rebleeding rate was reportedly significantly higher with ligation than with endoscopic obturation [25,26]. Thus, the application of endoscopic treatment alone as a curative treatment for FV is controversial, and subsequent additional treatment such as B-RTO may be required to acquire the long-term effect.

A model to predict survival in patients with an end-stage liver disease (MELD) scoring system is known as a predictive factor for prognosis of end-stage patients with liver cirrhosis [27–31]. However, the parameter of portal hypertension is not included in the calculation formula for this scoring. Ripoll et al. reported that inclusion of hepatic vein pressure gradient (HVPG) in MELD score variables for survival would help differentiate between the different types of patients with the same MELD score, because a more accurate prediction of survival was achieved when HVPG was included, with the result of 3% increase in death risk caused by a 1-mm Hg increase in HVPG [32]. Our result may also support the importance of portal hemodynamics to estimate the prognosis in patients with portal hypertension. In respect to this point, a major limitation of our study was the lack of information concerning PVP or HVPG, which may be closely related to the pathophysiology of the patient with portal hypertension. The relationship between these pressure data and prognosis after B-RTO is expected to be resolved in the near future. However, pressure measurement is more or less an invasive procedure that also requires radiation exposure. Although Doppler US could not demonstrate the pressure itself, the pre-treatment measurement of blood flow may allow a non-invasive assessment of the prognosis after B-RTO.

A second limitation may be that the blood flow measurement was done after the endoscopic treatments prior to B-RTO in 24 of the 44 bleeders, as they might have affected the portal hemodynamics. However, such cases are inevitable in clinical practice, and the relationship between portal hemodynamics just before B-RTO

and survival may be assessed in spite of the presence or absence of preceding treatments. The third was that approximately half of the patients received prophylactic B-RTO because of the patients' strong desire, though there was no randomized controlled trial regarding the efficacy of B-RTO for primary prophylaxis of FV bleeding. Our results would not justify the usage of B-RTO for primary prophylaxis for FV, and the application criteria of this technique needs to be established in further studies. Furthermore, as our study did not include control subject, that is untreated FV patients with HCC, poor liver function and/or GP-R equal to or more than 1.0 which were poor prognostic factor after B-RTO, significance of the application of B-RTO for the patients with these factors should also be investigated as a next challenge.

5. Conclusions

B-RTO provided a long-term therapeutic effect without recurrence for FV in cirrhotic patients. Poor prognosis after B-RTO was related to the development of HCC and severity of liver disease, and measurement of GP-R by Doppler US may be of value to obtain some indication regarding prognosis.

References

[1] Sarin SK, Lahoti D, Saxena SP, Murthy NS, Makwana UK. Prevalence, classification and natural history of gastric varices: a long-term follow-up study in 568 portal hypertension patients. Hepatology 1992;16(6):1343–9.

[2] Ryan BM, Stockbrugger RW, Ryan JM. A pathophysiologic, gastroenterologic, and radiologic approach to the management of gastric varices. Gastroenterology 2004;126(4):1175–89.

[3] Lubel JS, Angus PW. Modern management of portal hypertension. Intern Med J 2005;35(1):45–9.

[4] Williams SG, Westaby D. Management of variceal haemorrhage. BMJ 1994;308(6938):1213–7.

[5] Bosch J, Abraldes JG, Groszmann R. Current management of portal hypertension. J Hepatol 2003;38(Suppl. 1):S54–68.

[6] Kanagawa H, Mima S, Kouyama H, Gotoh K, Uchida T, Okuda K. Treatment of gastric fundal varices by balloon-occluded retrograde transvenous obliteration. J Gastroenterol Hepatol 1996;11(1):51–8.

[7] Koito K, Namieno T, Nagakawa T, Morita K. Balloon-occluded retrograde transvenous obliteration for gastric varices with gastrorenal or gastrocaval collaterals. AJR Am J Roentgenol 1996;167(5):1317–20.

[8] Hirota S, Matsumoto S, Tomita M, Sako M, Kono M. Retrograde transvenous obliteration of gastric varices. Radiology 1999;211(2):349–56.

[9] Ninoi T, Nishida N, Kaminou T, et al. Balloon-occluded retrograde transvenous obliteration of gastric varices with gastrorenal shunt: long-term follow-up in 78 patients. AJR Am J Roentgenol 2005;184(4):1340–6.

[10] Hiraga N, Aikata H, Takaki S, et al. The long-term outcome of patients with bleeding gastric varices after balloon-occluded retrograde transvenous obliteration. J Gastroenterol 2007;42(8):663–72.

[11] Chikamori F, Kuniyoshi N, Shibuya S, Takase Y. Eight years of experience with transjugular retrograde obliteration for gastric varices with gastrorenal shunts. Surgery 2001;129(4):414–20.

[12] Akahane T, Iwasaki T, Kobayashi N, et al. Changes in liver function parameters after occlusion of gastrorenal shunts with balloon-occluded retrograde transvenous obliteration. Am J Gastroenterol 1997;92(6):1026–30.

[13] The Japan Society for Portal Hypertension. The general rules for study of portal hypertension. 2nd ed. Kanehara & Co., Ltd.; 2004.

[14] Matsutani S, Furuse J, Ishii H, Mizumoto H, Kimura K, Ohto M. Hemodynamics of the left gastric vein in portal hypertension. Gastroenterology 1993;105(2):513–8.

[15] Maruyama H, Ishihara T, Ishii H, et al. Blood flow parameters in the short gastric vein and splenic vein on Doppler ultrasound reflect gastric variceal bleeding. Eur J Radiol, in press.

[16] Watanabe K, Kimura K, Matsutani S, Ohto M, Okuda K. Portal hemodynamics in patients with gastric varices: a study in 230 patients with esophageal and/or gastric varices using portal vein catheterization. Gastroenterology 1988;95(2):434–40.

[17] Maruyama H, Okugawa H, Yoshizumi H, Kobayashi S, Yokosuka O. Hemodynamic features of gastrorenal shunt: a Doppler study in cirrhotic patients with gastric fundal varices. Acad Radiol 2008;15(9):1148–54.

[18] Chikamori F, Kuniyoshi N, Kawashima T, Takase Y. Gastric varices with gastrorenal shunt: combined therapy using transjugular retrograde obliteration and partial splenic embolization. AJR Am J Roentogenol 2008;191(2):555–9.

[19] Quaia E. Microbubble ultrasound contrast agents: an update. Eur Radiol 2007;17(8):1995–2008.

[20] Goldberg BB, Hilpert PL, Burns PN, et al. Hepatic tumors: signal enhancement at Doppler US after intravenous injection of a contrast agent. Radiology 1990;177(3):713–7.

[21] Sarin SK, Jain AK, Jain M, Gupta R. A randomized controlled trial of cyanoacrylate versus alcohol injection in patients with isolated fundic varices. Am J Gastroenterol 2002;97(4):1010–5.

[22] Akahoshi T, Hashizume M, Shimabukuro R, et al. Long-term results of endoscopic histoacryl injection sclerotherapy for gastric variceal bleeding. A 10-year experience. Surgery 2002;131(Suppl. 1):S176–81.

[23] Takeuchi M, Nakai Y, Syu A, Okamoto E, Fujimoto J. Endoscopic ligation of gastric varices. Lancet 1996;348(9033):1038.

[24] Shiha G, El-Sayed SS. Gastric variceal ligation: a new technique. Gastrointest Endosc 1999;49(4 Pt 1):437–41.

[25] Lo GH, Lai KH, Cheng JS, Chen MH, Chiang HT. A prospective, randomized trial of butyl cyanoacrylate injection versus band ligation in the management of bleeding gastric varices. Hepatology 2001;33(5):1060–4.

[26] Tan PC, Hou MC, Lin HC, et al. A randomized trial of endoscopic treatment of acute gastric variceal hemorrhage: N-butyl-2-cyanoacrylate injection versus band ligation. Hepatology 2006;43(4):690–7.

[27] Malinchoc M, Kamath PS, Gordon FD, Peine CJ, Rank J, ter Borg PC. A model to predict poor survival in patients undergoing transjugular intrahepatic portosystemic shunts. Hepatology 2000;31(4):864–71.

[28] Kamath PS, Wiesner RH, Malinchoc M, et al. A model to predict survival in patients with end-stage liver disease. Hepatology 2001;33(2):464–70.

[29] McCaughan GW, Strasser SI. To MELD or not to MELD? Hepatology 2001;34(1):215–6.

[30] Wiesner RH, McDiarmid SV, Kamath PS, et al. MELD and PELD: application of survival models to liver allocation. Liver Transpl 2001;7(7):567–80.

[31] Freeman Jr RB, Wiesner RH, Harper A, et al. The new liver allocation system: moving toward evidence-based transplantation policy. Liver Transpl 2002;8(9):851–8.

[32] Ripoll C, Bañares R, Rincón D, et al. Influence of hepatic venous pressure gradient on the prediction of survival of patients with cirrhosis in the MELD Era. Hepatology 2005;42(4):793–801.

JOURNAL OF VIRAL HEPATITIS
JVH

Journal of Viral Hepatitis, 2010, **17**, 618–623 doi:10.1111/j.1365-2893.2009.01221.x

Hepatitis A virus (HAV) proteinase 3C inhibits HAV IRES-dependent translation and cleaves the polypyrimidine tract-binding protein

T. Kanda,[1] V. Gauss-Müller,[2] S. Cordes,[2] R. Tamura,[1] K. Okitsu,[1] W. Shuang,[1] S. Nakamoto,[1] K. Fujiwara,[1] F. Imazeki[1] and O. Yokosuka[1] [1]*Department of Medicine and Clinical Oncology, Graduate School of Medicine, Chiba University, Inohana, Chuo-ku, Chiba, Japan; and* [2]*Institute of Medical Molecular Biology, University of Lübeck, Lübeck, Germany*

Received July 2009; accepted for publication September 2009

SUMMARY. Hepatitis A virus (HAV) infection is still an important issue worldwide. A distinct set of viruses encode proteins that enhance viral cap-independent translation initiation driven by an internal ribosome entry site (IRES) and suppress cap-dependent host translation. Unlike cytolytic picornaviruses, replication of HAV does not cause host cell shut off, and it has been questioned whether HAV proteins interfere with its own and/or host translation. HAV proteins were coexpressed in Huh-7 cells with reporter genes whose translation was initiated by either cap-dependent or cap-independent mechanisms. Among the proteins tested, HAV proteinase 3C suppressed viral IRES-dependent translation. Furthermore, 3C cleaved the polypyrimidine tract-binding protein (PTB) whose interaction with the HAV IRES had been demonstrated previously. The combined results suggest that 3C-mediated cleavage of PTB might be involved in down-regulation of viral translation to give way to subsequent viral genome replication.

Keywords: 3C protease, hepatitis A virus, IRES, PTB, translation.

INTRODUCTION

The messenger-sense RNA genome of hepatitis A virus (HAV) is about 7500 nucleotides in length and contains a single large open-reading frame (ORF) encoding a polyprotein with the capsid proteins representing the amino-terminal third and the remainder comprising a series of nonstructural proteins required for viral RNA replication: 2B, 2C, 3A, 3B, $3C^{pro}$ (cysteine proteinase responsible for most post-translational cleavage events within the polyprotein) and $3D^{pol}$ (RNA-dependent RNA polymerase, see Fig. 1a, top panel) [1]. In a regulated cascade, the viral polyprotein is cleaved by $3C^{pro}$ into intermediate and mature products that fulfill distinct functions in the viral life cycle. At both ends of the picornaviral genome, the ORF is flanked by highly structured nontranslated regions (5′NTR and 3′NTR). The down-stream part of the 5′NTR presents an internal ribosome entry site (IRES) that allows translation by a cap-independent mechanism [1–3]. Several IRES trans-acting factors (ITAF) have been identified as mediating IRES binding to the ribosome [4]. Whereas glyceraldehyde-3-phosphate-dehydrogenase (GAPDH) and La autoantigen suppress HAV IRES activity, the poly(C)-binding protein (PCBP) and the polypyrimidine tract-binding protein (PTB) were found to enhance HAV translation [3,5–9]. PTB, a 57-kDa protein, is a member of the heterogeneous nuclear ribonucleoprotein family that shuttles between the nucleus and cytoplasm [10]. While experimental data have demonstrated PTB binding to polypyrimidine tracts (UCUUU or UCUUC) in picornaviral IRES, the exact cellular functions of PTB are as yet incompletely defined [3,10,11].

Proteolytic cleavage of host proteins is a common mechanism executed by picornaviruses to shut off host cell protein synthesis and to regulate viral protein and RNA synthesis. These two synthetic processes are central in the viral life cycle and mutually exclusive on the same RNA template. As HAV does not shut off host protein synthesis, it seems that HAV cap-independent translation constantly

Abbreviations: GAPDH, glyceraldehyde-3-phosphate-dehydrogenase; HAV, Hepatitis A virus; IRES, internal ribosome entry site; ITAF, IRES trans-acting factors; ORF, open-reading frame; PABP, poly(A)-binding protein; PCBP, poly(C)-binding protein; PTB, polypyrimidine tract-binding protein.

Correspondence: Dr Tatsuo Kanda, Department of Medicine and Clinical Oncology, Graduate School of Medicine, Chiba University, 1-8-1 Inohana, Chuo-ku, Chiba 260-8677, Japan. E-mail: kandat-cib@umin.ac.jp